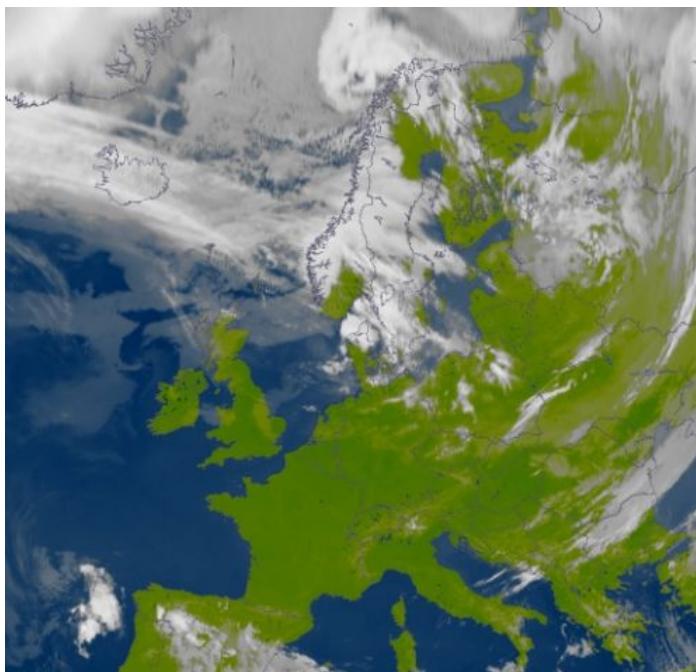# MEASURED, MODELLED AND SATELLITE DERIVED SOLAR RADIATION IN SCANDINAVIA

MASTER'S THESIS IN METEOROLOGY

LINDA HAGEN

JUNE 2011

UNIVERSITY OF BERGEN
GEOPHYSICAL INSTITUTE

Acknowledgements

Abstract

This article presents a comparison of global radiation data at different sites at the Scandinavian Peninsula. It makes use of ground truth, modelled and satellite derived surface global radiation data. First, a quality control of the ground truth data is conducted by evaluating measurements against the clear sky radiation estimated by a reliable model. Second, global radiation data derived from the geostationary satellite Meteosat are compared to the ground truth data.

The picture on the front page is a segment of a picture of Europe taken by the geostationary satellite Meteosat at 10.15 on March 23, 2011. The picture is downloaded from yr.no, which is an on-line weather service by the Norwegian Meteorological Institute and the Norwegian Broadcasting Corporation (NRK) (n.d.). The image is artificially coloured to better distinguish land, sea and clouds.

Contents

1 Introduction

Solar radiation is important for both the climate of the Earth and many purposes concerning a wide range of human activities, vegetation etc. In many cases it can be convenient to know the spatial and temporal distribution of solar radiation, especially in populated areas. Global radiation, the sum of direct and diffuse solar radiation on a horizontal surface, can be measured with an instrument called pyranometer. For financial reasons, the density of meteorological stations and thus solar radiation measurements, are limited.

To cover missing areas between stations, it has been developed several methods to estimate solar radiation. One way to obtain solar radiation data in areas beyond the range of measuring instruments is to use data derived from satellites. Output data with nearly continuous spatial and temporal coverage are available and are found to correspond well with ground truth data (Zelenka et al. 1999). To estimate hourly global irradiance at ground level, the method called Heliosat is applied where images from the visible channel (0.5 - 0.9 μm) of the geostationary satellite Meteosat is used as input. The Heliosat method was originally presented by Cano et al. (1986) and has been modified by various scientists since, including Beyer et al. (1996) and the EU-project Satel-Light Fontoynont et al. (1998). The Satel-Light team produced satellite derived global radiation and made it available in a database. Olseth & Skartveit (2001) compared satellite estimated solar radiation data to ground truth data from some European sites for the period 1996-1997. Now, satellite estimates for the period 1996-2000 are available in the database. Satellite derived global radiation for the whole period for some of the stations included here, has not been used prior to this study. At least according to what is known.

During recent years there has been an increased focus on climate and how it is developing. By being the driving force of the climate system, the sun and its radiant energy have been and always will be highly relevant. A number of publications on measured and satellite derived global radiation already exist, but many issues are yet to be fully covered. With increasing latitude, the geostationary satellite sees the surface at an increasingly unfavourable angle. Problems concerning this and the inability to separate snow from clouds are among the topics highlighted in this study but still require further work.

For satellite derived solar radiation data at the latitudes of Scandinavia, the issue concerning the geostationary satellites' increasingly unfavourable view of the Earths' surface is especially important. Some of the stations in this thesis, Umeaa and Ostersund for example, are located close to the maximum northern border of the surface area viewed by the satellite. The high latitudes and an unevenly sun-heated Earth, results in more snow, longer winters and a seasonal variation of day length in these areas. All of this combined, increase the difficulties with satellite estimates of solar radiation at high latitudes additionally.

Polar orbiting satellites on the other hand, are better suited at high latitudes. These satellites passes (or at least close to) both poles of the Earth, and can observe the entire

surface during a twelve hour period. The view of the surface of the Earth is therefore less unfavourable at high latitudes, but the data are not continuous in time. Polar satellites see different areas in the following passage.

This thesis is divided into five sections; section one gives a brief introduction to the topic. Then there is some basic theory about solar radiation and information about the general climate of Scandinavia in section two. Section three contains information about the ground truth data from eleven Scandinavian stations (six Norwegian and five Swedish) from the years 1996-2000 and the models used to estimate solar radiation. Section four provides results and interpretations, where both the quality control and the comparison of observed and satellite-derived solar radiation are evaluated. In the fifth and last section, summary and conclusions are given.

2 Theory

The first part of this chapter presents some general information about solar radiation. On the way from its source to the surface of the Earth, solar radiation might be affected by several processes and these are discussed in this part of the thesis. A brief description of the parameters affecting the solar radiation is also given. This is followed by some relevant information about the study area in the last subsection.

2.1 Solar radiation

The sun is the energy source to sustain life on Earth (Hartmann 1994). The distance from the energy source determines the time Earth spend orbiting the sun one full round and defines the length of one year as we know it (one planetary year). The distance also determines the solar energy flux density, the amount of solar energy delivered per unit time per unit area, which decreases with increasing distance from the source (figure 1). Because of the large distance from the energy source, the solar radiation flux density at the top of the atmosphere of the Earth is weakened. The intensity of the radiation has not been reduced but rather spread over a larger area.
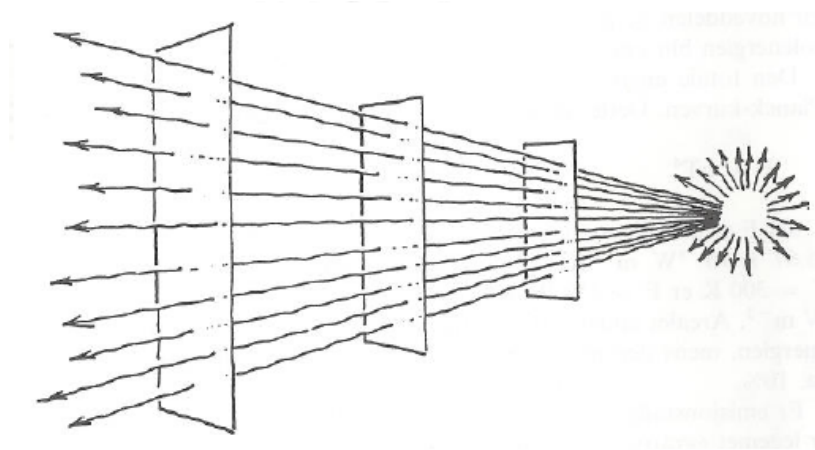
Figure 1: The intensity of the radiation energy decrease with increasing distance from the energy source. It is the same amount of energy, but distributed over a larger area. The figure is taken from Utaaker (1991).

The amount of solar radiation reaching the outer boundary of the atmosphere is assumed constant and is called the solar constant (S_0). It is defined as the solar flux density on a surface normal to the solar rays at the mean sun-earth distance. According to Hartmann (1994), S_0 is given as

$$S_0 = \frac{L_0}{4\pi d^2} = 1367 \ \mathrm{Wm}^{-2} \tag{1}$$

where

$$L_0 = 3.9 * 10^{26} \text{ W} \tag{2}$$

$$d = 1.5 * 10^{11} \text{ m} \tag{3}$$

L_0 is the solar luminosity and d is the mean distance between the sun and the earth.

The orbit of the Earth about the sun is elliptic and the eccentricity is a measure of how much the elliptic orbit deviates from a circle. Parameters of the rotation of the Earth and their relationship to the orbit, also affect the amount of solar radiation received at the surface.

In addition to orbiting the sun, Earth rotates about its own axis. One round is what we know as one day, so the rotation gives a diurnal cycle. The seasonal variation of insolation at our latitudes, is mainly influenced by the angle between the axis of rotation and the normal to the plane of the orbit. This tilt is called the obliquity and is currently about 23.45°.

The point in the orbit of the Earth about the sun where the Sun-Earth distance is at a minimum is called perihelion and happens approximately at January 5. This is during the Southern Hemisphere summer and results in more insolation at the top of the atmosphere at Southern than in the Northern Hemisphere summer.

2.1.1 Global solar radiation

The insolation received by a measuring instrument is commonly known as global radiation (H_g). The total solar radiation on a horizontal surface from all solid angles in a hemisphere is the sum of the two components, direct (H_b) and diffuse (H_d) radiation

$$H_g = H_b + H_d \tag{4}$$

where

$$H_b = H_{bnormal}cos(\theta) \tag{5}$$

with $H_{bnormal}$ as the direct radiation normal to the incoming solar radiation and θ as the solar zenith angle. While the direct component (H_b) is the radiation beam coming through the atmosphere without being affected, the diffuse component (H_d) is the solar radiation scattered before reaching the surface. See section 2.1.4 for more information about atmospheric radiation processes and the diffuse component.

All matter emit electromagnetic radiation. The emission of an object depends on its temperature and it emits at decreasing wavelength with increasing temperature (Hartmann 1994). The surface temperature of the sun is approximately 6000K, which results in a radiant energy output of the sun approximately between wavelengths of 0.1 μm and 4 μm. The radiation reaching the surface of the Earth consists mainly of

- Ultraviolet radiation (UV, 0.28 - 0.4 μm)

- Visible radiation (0.4 - 0.75 μm)

- Near infrared radiation (0.75 - 4 μm)

This is why solar radiation is often called short-wave radiation. Of the total radiation amount emitted from the sun, 99 % is in the range 0.25 - 4 μm and approximately 95 % is in the range 0.3 - 2.4 μm according to Iqbal (1983). Ultraviolet radiation makes up a small fraction of the radiation reaching the surface (where the shortest wavelengths are absorbed before reaching the surface), but it is still important.

UV radiation can change chemical structures, which has both negative and positive aspects. It is negative in the way that it might be harmful to life. Despite this, it also contributes to formation of vitamin D in the human skin. Vitamin D is a nutrient important to ensure the absorption of calcium necessary for a healthy skeletal. Except from food as milk and butter, which in some cases is artificially added vitamin D, fish and solar radiation is the only natural sources. At high latitudes the solar radiation is low or even absent during parts of the winter, and this reduces the available vitamin D dramatically.

2.1.2 Solar geometry

Relevant parameters for the sun-earth geometry are included below.

- The solar elevation (h)

  The angle between the centre of the disc of the sun and the horizon. See figure 2, which is a modified version of a illustration from a solar calculator glossary by National oceanic & atmospheric administration (NOAA).

- The solar zenith angle (θ)

  The angle between a local normal to the surface of the Earth and a line between a point on the surface of the Earth and the sun. $h + \theta = 90°$.

- The solar azimuth angle (φ)

  The angle between the projection of the normal to a surface onto the horizontal and true north. Measured clockwise.

- The solar declination (δ)

  The angle between equator (E) and a line drawn from the centre of the Earth to the centre of the sun. It varies between $23.45°$ at northern summer solstice to $-23.45°$ at northern winter solstice. See figure 3, which is a modified version of a illustration from a introductory lecture by Bairstow.
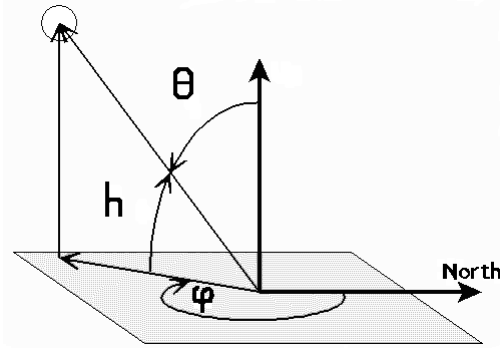
Figure 2: The solar elevation (h), solar zenith angle (θ) and solar azimuth angle (φ).
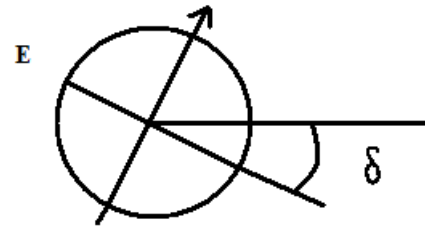
Figure 3: The solar declination angle (δ) at northern summer solstice.

- The solar hour angle (ω)

  The angle which the Earth need to rotate to locate the longitude of a given point directly under the sun.

According to Hartmann (1994), the cosine of the solar zenith angle can be derived for any latitude (ϕ), season and time of day with these definitions.

$$sin(h) = cos(\theta) = sin(\phi)sin(\delta) + cos(\phi)cos(\delta)cos(\omega) \tag{6}$$

When the sun is below the horizon and darkness prevails, equation 6 is negative. A solar zenith angle at $90°$ corresponds to a sun which either is rising or setting.

2.1.3   Parameters affecting the solar radiation

It is important to understand which parameters and how they are affecting the global radiation. A short presentation of the important parameters are given in this subsection.

- The solar elevation

  Low solar elevations results in a longer atmospheric path for the beam. There is a larger probability of being scattered or absorbed in the atmosphere, so the transmitted solar radiation at the surface will be lower. This results in decreasing solar radiation with increasing latitude. Besides, in addition to a lower $H_{bnormal}$ (equation 5), $cos(\theta)$ is also lower at low sun.

- Clouds

  Of all the atmospheric parameters affecting the global radiation, the clouds are most important. The amount and type vary from place to place, and causes variations in surface global radiation on different time scales. A totally covered sky with clouds which are dense and have a large vertical extent, extinct more of the global radiation than a thinner cloud. Clouds of sufficient thickness are effective reflectors of solar radiation and this tends to cool Earth. Short wavelengths as UV are less reduced by clouds than say visible radiation.

- Albedo

  Another factor which is affecting the solar radiation received by instruments measuring global radiation, is the surface reflectivity or the surface albedo. With increasing reflection of solar radiation the albedo increase. Albedo is expressed in percent or on a scale from 0 to 1 where 0 represent no reflection and 1 is completely reflected (the latter alternative is chosen here).

  The effects of albedo on measured and modelled global radiation on a horizontal surface depends on the topography and the cloud situation. If clouds and/or elevated topography are present, the albedo is important. Clouds increase the backscattered radiation, snow-covered mountains increase the reflection from the topography, both of which increase the global radiation. The albedo is less important in clear sky situations in areas with low topography, where the backscattered radiation from the atmosphere with low albedo is small.

- Ozone

  The stratosphere contains approximately 90 % of the total amount of this parameter. Due to human activities such as industry and transportation with the corresponding pollution, the ozone amount has increased in the troposphere during the past several decades. Originally most of the atmospheric ozone are formed where the solar radiation is most intense, which is in the tropic stratosphere, before being transported by the winds to the north and the south. By absorbing most of

the short-waved UV radiation that otherwise would reach the surface, the ozone layer is protecting life on earth.

- Turbidity

  Turbidity is an optical parameter of the atmosphere affecting the global radiation. An enhanced amount of particles suspended in the air, also called aerosols, increases this parameter. According to Iqbal (1983), the presence of aerosols in the atmosphere can be quantified by the number of dust particles per cubic centimetre, atmospheric turbidity and visibility. Aerosols are either of terrestrial or marine origin and vary in volume, size, form, distribution and material composition. A variety of aerosols affect the transmission of solar radiation.

All of the parameters listed above except clouds are used as input when modelling global radiation. Clouds are excluded because the model produces an estimate of clear sky radiation. Despite this, it is important to know how clouds are affecting the surface solar radiation. The clear sky model and input parameters are discussed further in chapter 3.2.1.

2.1.4 Radiation processes in the atmosphere

The amount of solar radiation penetrating through atmosphere and reaching the surface of the Earth varies geographically and seasonally, depending on the distribution of insolation and the atmospheric condition. Generally, low latitudes are exposed to more insolation than polar areas (see explanation in section 2.1). This combined with different cloud characteristics and varying climatological averages of meteorological parameters as ozone and water vapour, results in the varying surface solar radiation.

When a photon on its way to the surface of the Earth encounters the atmosphere, several interactions are possible.

- *Transmission* is the first alternative and represent situations where the photon passes through the atmosphere without being affected.

- A change in direction is also likely to happen, and this process is referred to as *scattering.*

- The last alternative is *absorption*, where the energy of the photon will be transferred to the atmosphere.

Scattering and absorption combined, constitute what is called *extinction.*

As shown in figure 4, the solar irradiance received at sea level in clear sky situations has a spectral distribution. The energy curve for a black body with a temperature at 5250 °K and the solar irradiance curve at the top of the atmosphere are also given. The gaseous absorption bands are specified.
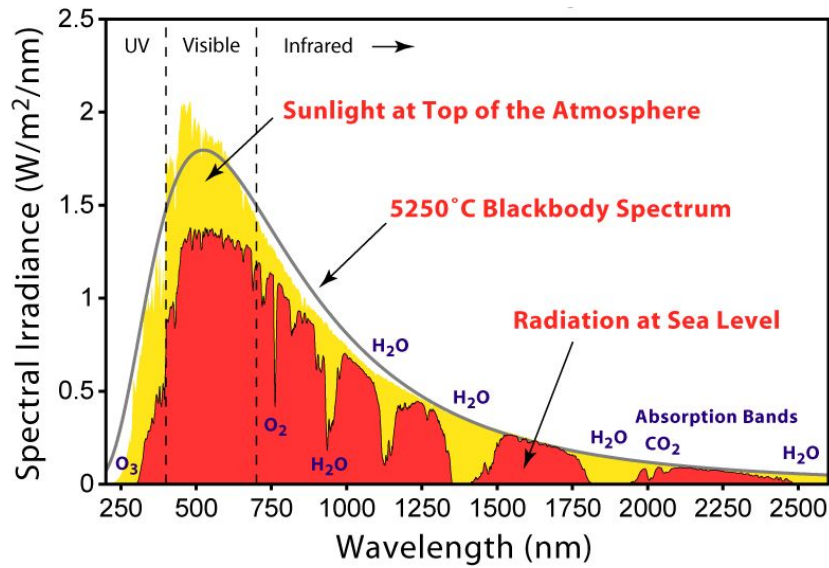
Figure 4: Spectral energy curve for a blackbody at 5250 °K (smooth solid line), the solar radiation outside the atmosphere (the bright coloured area) and at sea level (the darker coloured area). The gaseous absorption bands are specified. The image is created by Robert A. Rohde, Global Warming Art (2007).

The emission peak of the sun at approximately 0.6 μm (600 nm) and the three wavelength groups that the solar energy normally are divided into (UV, visible and near infrared) were discussed in section 2.1.1, but are shown graphically in figure 4. The most harming UV-radiation is absorbed by the ozone (O_3). Other than this, water vapour (H_2O) and carbon dioxide (CO_2) are especially absorbing infrared radiation.

Depending on the size of the particles which the radiation encounters, there are two important alternatives of scattering. Scattered radiation where the particles are small compared to the wavelength is called "Rayleigh scattering" and where particles are larger compared to the wavelength are called "Mie scattering". Radiation scattered in the former case are scattered approximately equally forward and backwards, while the latter is mainly scattered forward.

2.2 Climate in Scandinavia

Generally, the climate in Scandinavia is characterized as mild. This is relative to the geographical location at high latitudes. The Gulf Stream origins in the areas close to Florida and is a powerful and warm ocean current which transport warm water masses across the Atlantic Ocean. Weather systems drifting into Northern Europe and hitting the Norwegian coast are heated by the Gulf Stream before heating the climate at these latitudes. Despite being close to the Arctic territories, most of the Norwegian coast are free of snow and ice throughout the year.

According to Utaaker (1991), the following three factors are affecting the characteristics of the local climate

- The large-scale weather and climate conditions

- The surface types present in the area

- The topography in the area

The frequency and duration of the different large-scale weather conditions have a huge impact on the local climate. For cloud free situations with weak wind the climate is heavily affected by the radiation, while for cloudy and turbulent weather the climate is affected by the air masses transported into the area. This combined with the surface types (see discussion below) and topography in the area, results in a large variation in the local climates.

Despite the moderate size of Scandinavia, the topography and surface types varies a lot. The surface types and conditions affect the surface albedo, which varies both locally and regionally. Most surfaces have a stable albedo on a daily and yearly basis. Typical values ranges from as little as 0.05 to as much as 0.90, where most natural surfaces has albedo less than 0.30. Fresh, dry snow is among the surfaces which have the largest albedo, while water surfaces under light winds have among the lowest values. Table 1 gives a short overview of characteristic values of different surface albedo important when working with data from Scandinavian locations and climate.

Table 1: Albedo for selected surfaces, both range and typical values are given. The values presented in the table are from Hartmann (1994).

Surface	Range	Typical value
Fresh, dry snow	0.70-0.90	0.80
Old, melting snow	0.35-0.65	0.50
Forest with surface snow-cover	0.20.0.35	0.25
Short green vegetation	0.10-0.20	0.17
Deep water: high wind, low altitude	0.10-0.20	0.12
Coniferous forest	0.10-0.15	0.12
Deep water: low wind, high altitude	0.05-0.10	0.07

As discussed in section 2.1.3, there are several parameters which can affect the solar radiation climate in Scandinavia. One of these is the solar elevation, which is giving a strong seasonal change in the length of day and night at these latitudes. In the southern parts of Norway and Sweden, the sunshine duration varies dramatically from midsummer to midwinter. Areas north of the Arctic Circle have a period with prevailing sunlight midsummer and darkness midwinter. These phenomena are called Midnight sun and Polar night.

Figure 5 shows the modelled path of the sun across the sky for the twenty-first day of the months March, June and December for the two Norwegian stations Skogmo (dashed line) and Landvik (fully drawn line). Skogmo is situated at 64.51°N and 12.02°E and Landvik is situated at 58.34°N and 8.52°E. Despite a small difference of approximately 6° in latitude, the solar elevation at solar noon is significantly lower at Skogmo than at Landvik.

Mostly because of the solar elevation differences, the clear sky global radiation also differs. At latitudes further north, the modelled clear sky global radiation at solar noon is lower. This is shown in figure 6, where the modelled clear sky curve for Skogmo (dashed line) and Landvik (fully drawn line) are given.

The total amount of atmospheric ozone varies with season and latitude. There is a yearly cycle in monthly ozone amounts with maximum during spring and minimum during autumn. This is shown in figure 7 (based on data from Iqbal (1983)) for the latitudes 60°N (fully drawn line) and 70°N (dashed line). In addition to this seasonal variation, the ozone amount also varies on a day to day basis which is not revealed by long-term averages such as the yearly cycle. If all the gaseous ozone in a vertical column of unit area were moved to normal temperature and surface pressure (NTP), the thickness of the resulting layer characterizes the total amount of atmospheric ozone (cm).

As mentioned in section 2.1.3, there are some seasonally and geographically differences in the turbidity. On average, the impact of the aerosol amount is highest during summer and lowest during winter. Summer months have typically a larger amount of atmospheric particles which is whirled up from a dry surface by the wind, compared to winter months. In addition, continental air contains smaller particles than marine air.

When discussing the climate of a location, it is important to look at statistics of the temperature and precipitation. These parameters give a good indication of the climate of a site. Figure 8 - 9 contains the normal temperature for the period 1961-1990 at eleven Scandinavian sites (six Norwegian and five Swedish), located on the west coast, inland and east coast of the Scandinavian Peninsula. The normal value of the precipitation for the period 1961-1990 for the same sites as the stations with temperature data, is presented in figure 10 - 11 (see section 3.1 for more information about the stations and the location).

As shown in figures 8 and 9, the temperature differs most from station to station during
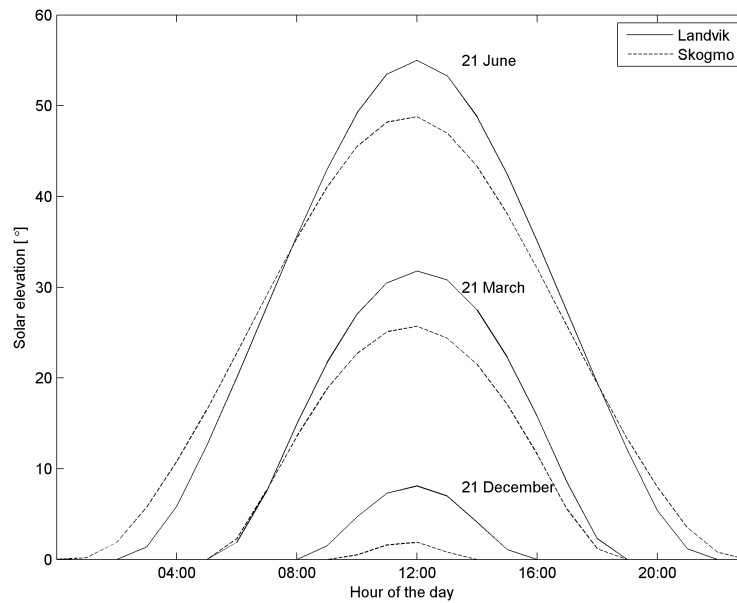
Figure 5: Modelled sun path at Skogmo (dashed line) and Landvik (fully drawn line) for 21 March, 21 June and 21 December.
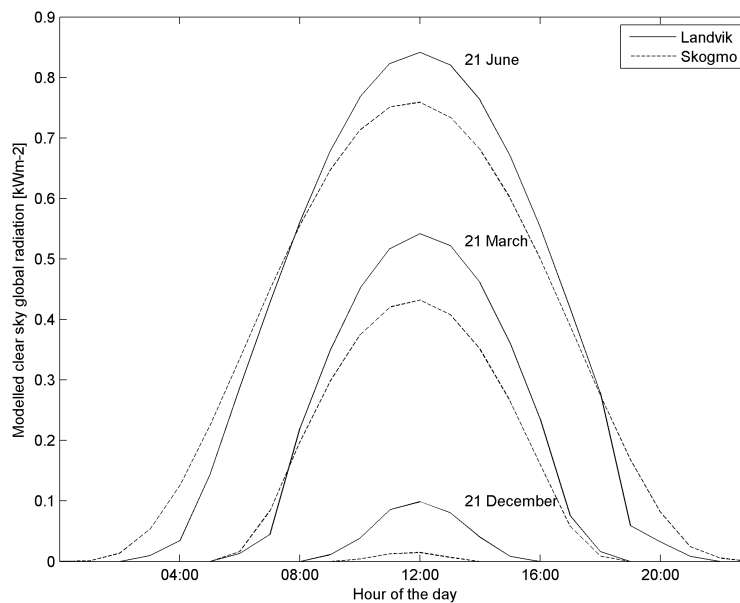

Figure 6: Modelled clear sky global radiation at Skogmo (dashed line) and Landvik (fully drawn line) for 21 March, 21 June and 21 December.
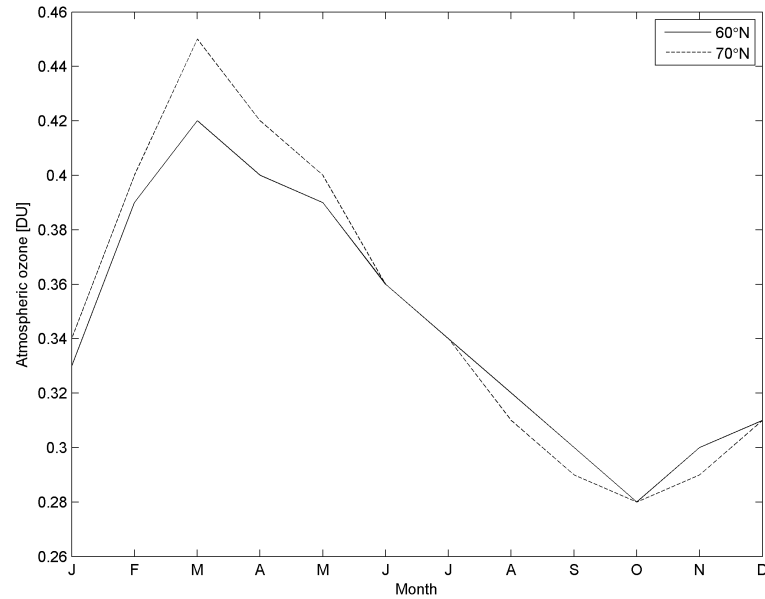
Figure 7: Seasonal variation of atmospheric ozone [cm(NTP)] for 60°N (fully drawn line) and 70°N (dashed line). Based on data from Iqbal (1983).

winter. The Norwegian sites Bergen and Fureneset are the only stations with an average temperature above zero during the coldest winter months (January and February). This is also the case in December, only here Landvik also has an average temperature slightly above zero. Of all the stations, Bergen has the highest annual normal temperature with 7.6°C and Ostersund has the lowest annual mean with 2.5°C.

Figures 10 and 11 show the precipitation amount for each of the eleven stations. Generally, the variation of precipitation amount from month to month is larger than for temperature. For both the Norwegian and Swedish stations, the precipitation amount is largest during the last part of the year, typically between July and November. In addition of the largest monthly precipitation amount, Bergen and Fureneset have the largest annual normal precipitation amount with 2250 mm and 2010 mm, respectively. Ostersund and Kise are the driest stations with 484.2 mm and 585.9 mm as normal precipitation amount (based on the normal period 1961-1990) on an annual basis.

Temperature and precipitation data from the Norwegian stations (in figure 8 and 10) are downloaded from *eKlima, a web portal which gives free access to the climate database of the Norwegian Meteorological Institute* (n.d.). Data from the Swedish stations (in figure 9 and 11) are downloaded from *smhi.se, the on-line climate database of the Swedish Meteorological and Hydrological Institute* (n.d.). See section 3.1 for more information about the sites and the data.

14
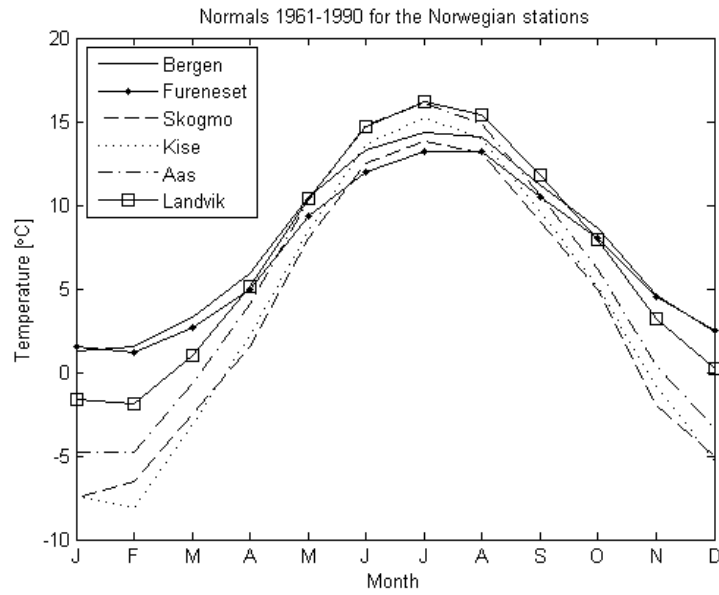
Figure 8: Monthly average temperature (°C) for the Norwegian stations Bergen, Fureneset, Skogmo, Kise, Aas and Skogmo. The averages are based on date from the normal period 1961-1990.

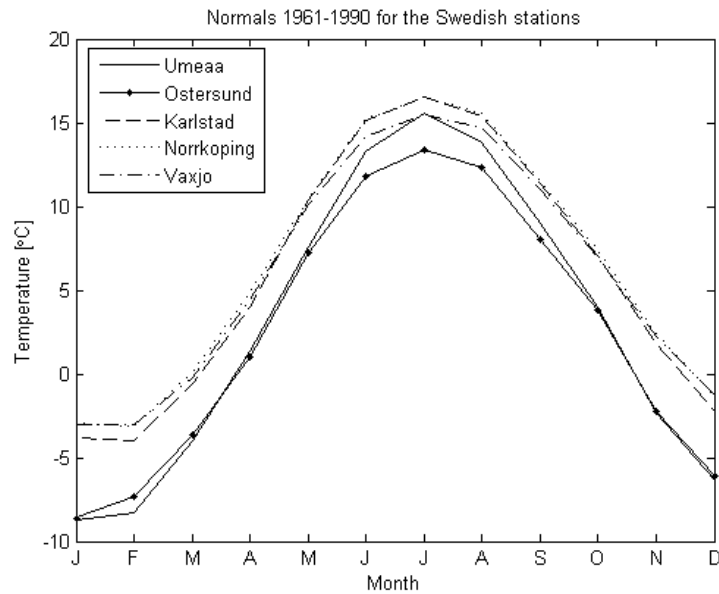Figure 9: Same as figure 8, for the Swedish stations Umeaa, Ostersund, Karlstad, Norrkoping and Vaxjo.
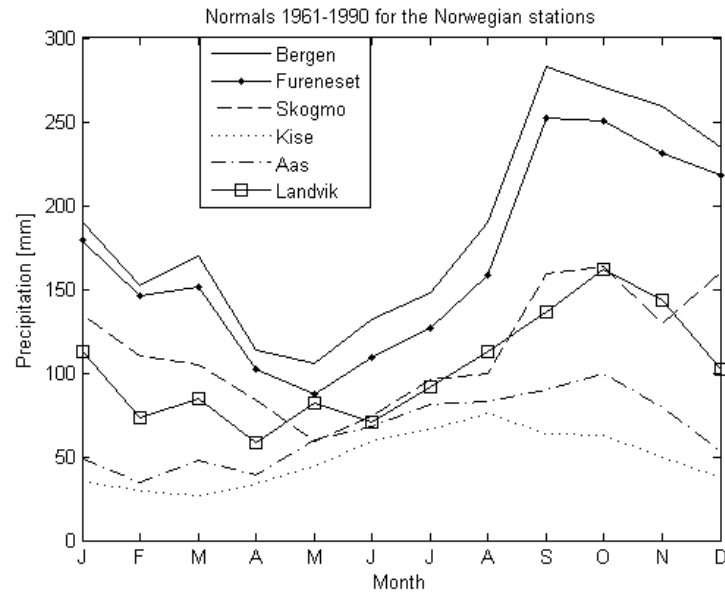
15

Figure 10: Monthly average precipitation (mm) for the Norwegian stations Bergen, Fureneset, Skogmo, Kise, Aas and Landvik. The averages are based on date from the normal period 1961-1990.
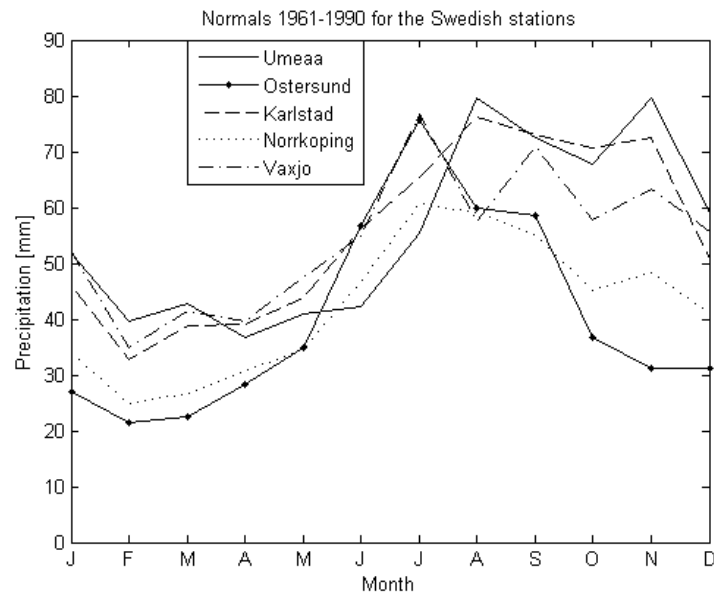

Figure 11: Same as figure 11, for the Swedish sites Umeaa, Ostersund, Karlstad, Norrkoping and Vaxjo.

16

3 Data and methods

Solar radiation can be measured, modelled by a radiative transfer model or derived from satellite measurements. The location of the meteorological stations, the measuring instrument, the model used to estimate global radiation and a procedure which derives solar radiation from satellite pictures, are described in this chapter.

3.1 Ground truth data

Out of all the meteorological observation stations in Scandinavia recording hourly global radiation, data from eleven stations in the southern part of the Scandinavian Peninsula are gathered from different sources and evaluated. Six stations are Norwegian and five are Swedish (see table 2 and figure 12).

Table 2: Station nationality, latitude (ϕ), longitude (λ) and meters above mean sea level (m.a.m.s.l.) of eleven Scandinavian sites for the period 1996-2000. The instrument positions are specified, where M represent ground level (approximately two meters above ground) and T represent roof.

Station	Country	Latitude (ϕ) [°N]	Longitude (λ) [°E]	Elevation [mamsl]	Position
Vaxjo	Sweden	56.93	14.73	182	M
Landvik	Norway	58.34	8.52	6	M
Norrkoping	Sweden	58.58	16.15	43	T
Karlstad	Sweden	59.36	13.47	46	M
Aas	Norway	59.66	10.78	89	M
Bergen	Norway	60.38	5.33	12	T
Kise	Norway	60.77	10.81	128	M
Fureneset	Norway	61.29	5.04	7	M
Ostersund	Sweden	63.20	14.50	376	T
Umeaa	Sweden	63.82	20.25	10	T
Skogmo	Norway	64.51	12.02	60	M

As shown in table 2 and the map in figure 12, the geographical location of the stations vary from 56° to 65°N in latitude and from 5° to 21°E in longitude. There is a great deal of variation in the location of the eleven sites. Stations are mainly scattered along the west and east coast of the Scandinavian Peninsula, but there are also some located inland and away from the coast. Station elevation ranges from approximately mean sea level and up to almost 400 meters above this level. Station nationality and position of the instruments are also specified in the table. A majority of the instruments are included on an installation near the ground (2m, M), while others are located on a roof (T).
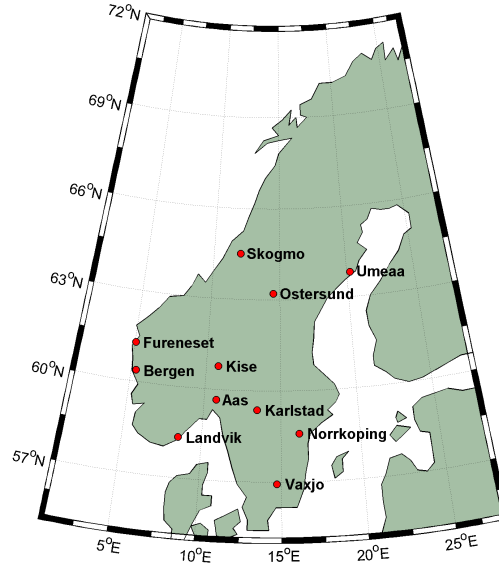
Figure 12: Map with geographical position of six Norwegian stations (Landvik, Aas, Bergen, Kise, Fureneset and Skogmo) and five Swedish stations (Vaxjo, Norrkoping, Karlstad, Ostersund and Umeaa).

Table 3: Relevant meteorological parameters available for each of the stations for the period 1996-2000. Global radiation (H_g), direct radiation (H_b), diffuse radiation (H_d), long-wave radiation (L), sunshine duration (SD), temperature (T), relative humidity (RH) and air pressure (p). "X" represent available and "-" represent unavailable.

Station	H_g	H_b	H_d	L	SD	T	RH	P
Vaxjo	X	-	-	-	X	X	X	-
Landvik	X	-	-	-	X	X	X	X
Norrkoping	X	X	X	X	X	X	X	X
Karlstad	X	-	-	-	X	X	X	-
Aas	X	-	-	X	-	X	X	-
Bergen	X	X	X	X	X	X	X	X
Kise	X	-	-	-	X	X	X	-
Fureneset	X	-	-	-	X	X	X	-
Ostersund	X	-	-	-	X	X	X	-
Umeaa	X	-	-	-	X	X	X	-
Skogmo	X	-	-	-	-	X	X	-

18

Table 3 gives an overview of the meteorological parameters recorded at each of the stations and are discussed further in the respective sections.

3.1.1 "Bioforsk"

The Norwegian Institute for Agricultural and Environmental Research (called "Bioforsk") is a research institute which performs research linked to agriculture, plant sciences and environmental protection. They focus on innovation, economic growth and sustainable resource use and work towards being a regional, national and international competitive producer of knowledge, services and solutions within plant production, food quality and environmental questions (the web page of *"Bioforsk"*, www.bioforsk.no).

Even though measuring solar radiation is not of great priority for this institute, around fifty of their over ninety stations have instruments collecting solar radiation data. Bioforsk deliver measurements from five of the six Norwegian stations in this thesis, and the stations of interest are Aas, Fureneset, Kise, Landvik and Skogmo. Measurements of global radiation started in 1987 at Fureneset, Kise and Landvik, while measurements at Aas and Skogmo started in 1991.

For all of these Bioforsk-stations, global radiation were recorded by a Kipp & Zonen CM11 pyranometer located on a installation near ground level (approximately two meters height) and is recorded in local standard time (LST = UTC + 1). A CM1 pyranometer was operating at Kise until 18.08.1998, but was then replaced by a CM11 pyranometer. At Skogmo, the instrument installation was replaced during July 1998.

In addition to measuring global solar radiation (H_g), all stations are equipped with instruments measuring sunshine duration (SD, except from Aas and Skogmo), temperature (T) and relative humidity (RH). Landvik also records pressure (P) and Aas long-wave terrestrial radiation (L).

3.1.2 University of Bergen

Global radiation measurements from the Norwegian station Bergen are delivered by Geophysical Institute, University of Bergen. A Kipp & Zonen CM11 pyranometer is installed on the roof of the Institute and is recording the global radiation in true solar time (TST). This site has been operating since 1952 and has been recording solar radiation data since 1965.

Bergen might be characterized as an advanced station and all the parameters listed in table 3 are recorded here.

3.1.3 Swedish Meteorological and Hydrological Institute

Solar radiation data from the five Swedish stations are delivered by the Swedish Meteorological and Hydrological Institute (SMHI). SMHI has approximately 100 meteorological stations covering Sweden; sixteen of those are recording global radiation. Data from Umeaa, Ostersund, Karlstad, Norrkoping and Vaxjo are used in this work.

In Karlstad and Vaxjo the measuring instrument is installed on a ground level mast (approximately at two meters). In Umeaa, Ostersund and Norrkoping the measuring instrument is placed in roof level. All but one of these stations are characterized as simple stations and are equipped with instruments measuring sunshine duration (SD), global radiation (H_g), temperature (T) and relative humidity (RH). The only exception is the advanced station Norrkoping which in addition to SD, H_g, T and RH is recording long-wave terrestrial radiation (L), direct radiation (H_b), diffuse radiation (H_d) and air pressure (p). An overview of the relevant parameters recorded at the Swedish stations were presented in table 3 in section 3.1.

For all of the Swedish stations, measurements have been recorded since 1983. There exists older measurements of solar radiation, but they are not directly compatible with those recorded after 1983. The reason is that stations have been moved and instruments replaced, and this gives a systematic difference which is not yet clarified. The data are recorded in local standard time (LST), which also in this case represent coordinated universal time (UTC) plus 1 hour (LST=UTC+1). The instrument used to record global solar radiation is a Kipp & Zonen CM11 pyranometer.

Since ground truth data are collected by different instruments depending on the responsible Institute, a quality control of the measured global radiation is necessary. The routines and extent of daily and periodic inspection and maintenance might differ from stations to station. The results of this quality control are presented in chapter 4.1.1.

3.1.4 Instrumentation

Instruments measuring short-wave solar radiation incident on a surface are called pyranometers. If installed horizontally, it is recording global radiation (direct and diffuse). The Norwegian and Swedish meteorological stations in this thesis are equipped with Kipp & Zonen CM11 pyranometers. The measurements are according to standards of the World Meteorological Organization (WMO), which is a specialized agency of the United Nations.

Figure 13 is taken from the instruction manual by Kipp & Zonen (2000) and shows a cross section of a CM11 pyranometer. As seen from the picture, the pyranometer consists of two glass domes (outer and inner) which is protecting the sensing element from external parameters as wind and rain, which easily can affect the temperature. The glass domes are translucent to radiation with wavelengths from 0.3 to 3 μm. Without these glass domes, the sensing element would have absorbed the all-wave radiant energy since it

is non-selective to the spectral distribution. In addition, the two glass domes prevents error due to long-wave radiation. A heated dome would emit long-wave radiation and affect the measurements.

Close to the sensing element there is located a compensation element, and the temperature difference between these two gives a measure of the intensity of the incoming solar radiation. The dessicator prevents the formation of dew on the inner side of the domes, which in some cases can cool down. There are also other pyranometer models which might have a different set-up within the instrument.
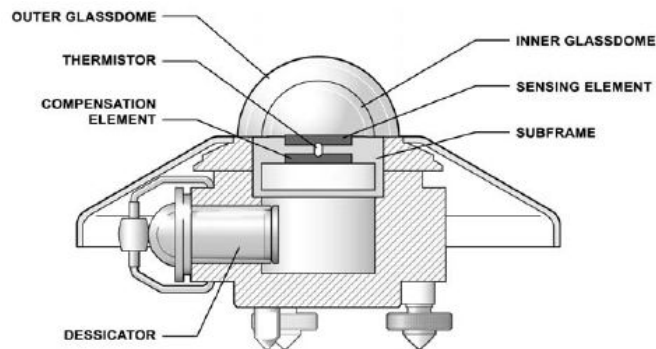
Figure 13: Cross-section of a Kipp & Zonen CM11 pyranometer. Main elements as outer and inner dome, sensing element and compensation element are specified.

Basically the pyranometer demand little maintenance. The outer dome should be cleaned and inspected e.g. every morning, whereas general conditions including cable conditions should be checked regularly. Dew or frost can be precipitated on the top of the outer dome and can stay there for hours, especially during cold season when such conditions can be expected. A periodic check should assure that the levelling of the instrument is horizontal. Other than this, an incorrect calibrating can be a potential source of error. According to a Kipp & Zonen CM series fact sheet, the expected daily accuracy is $\pm$ 3 %.

In addition, the pyranometers at the Swedish stations and the instrument in Bergen are ventilated. This means a blower is installed to keep the dome above dew point temperature to prevent dew formation. Snow is also more easily removed. The need for ventilation depends on local climatologically conditions and are useful at these latitudes during cold seasons.

3.2 Modelled solar radiation

To be able to evaluate the quality of measured global radiation, the clear sky index k_g can be calculated for a particular period. Normally this is obtained by dividing the measured global radiation H_g by the extraterrestrial global irradiation. Instead, we divide by an average clear sky irradiation H_0

$$k_g = \frac{H_g}{H_0} \tag{7}$$

where the parameters H_g and H_0 depends on the solar elevation. This solar elevation dependency is approximately removed by inserting these parameters into a fraction. The clear sky radiation (H_0) is obtained by running a broad band model, which in this case is the McMaster Model (Davies & McKay (1982)). The clear sky global radiation (H_0) is the sum of direct beam (H_{b0}) and diffuse radiation (H_{d0}) from both Rayleigh scattering (H_{doR}) and from scattering by aerosols (H_{doA})

$$H_0 = H_{b0} + H_{d0} = H_{b0} + H_{doR} + H_{doA} \tag{8}$$

where the components are defined as

$$H_{b0} = S cos\theta [T_r(0)T_r(R) - a_w]T_r(A) \tag{9a}$$

$$H_{doR} = \frac{S cos\theta T_r(0)[1 - T_r(R)]}{2} \tag{9b}$$

$$H_{doA} = S cos\theta [T_r(0)T_r(R) - a_w][1 - T_r(A)]\omega_0 f \tag{9c}$$

Here, the parameters are

- S : the solar constant corrected for the departure of the actual sun-earth distance from the mean value

- θ : solar zenith angle

- $T_r(0)$: the transmissivity after absorption by ozone

- $T_r(R)$: the transmissivity after Rayleigh scatter

- $T_r(A)$: the transmissivity after extinction by aerosols

- a_w : the absorptivity of water vapour

- ω_0 : the spectrally-averaged single scattering albedo for aerosols

- f : the ratio of forward to total scattering by aerosols

3.2.1   Input parameters to the McMaster model

The model is run for the period 1996-2000, from which satellite data exists. For each of the stations the following parameters are used as input to the model

- The position of the sun

  Can be derived by equation 6 (section 2.1.2) from latitude (ϕ), longitude (λ), day of the year and hour of the day. The two parameters ϕ and λ are given for each station in table 2. The calculations are done for 24 hours and 365 days.

- Horizon-panorama:

  If available, as it is for the Norwegian stations, thirty-six elevation angles in the directions from 10° - 360° azimuth are added. An unobstructed free horizon (with elevation angle 0° in all thirty-six directions) is the input horizon data for the Swedish stations. It is also specified that the horizon elevation vary linearly with azimuth by accepting a linear interpolation.

- Air pressure (in hPa):

  Since the station elevation ranges from 6 to 376 meters above mean sea level (m.a.m.s.l. or z in this case), the average air pressure vary from station to station. The effect of this variation is small, but is taken into consideration. Air pressure is estimated from station elevations (table 2 in section 3.1) by the equation

$$p = 1013 \exp(-0.1188z - 0.00116z^2) \tag{10}$$

  which is taken from Paltridge and Platt (1976).

- Monthly precipitable water vapour amounts (cm):

  This parameter is derived from surface dew point temperature by using the equation

$$w = \exp(0.07 * T_D - 0.075) \tag{11}$$

  which is taken from Perez et al. (1990). The values 0.07 and 0.075 are seasonal constants for the latitude 60.

  For the stations Landvik, Furenestet and Kise, w is calculated from records of monthly average dew point temperature based on two to four years. If neither precipitable water vapour nor surface dew point temperature data exist, w can be calculated from records of average air temperature and relative humidity. This is the case for the Norwegian stations Aas and Skogmo, and all the Swedish stations. To convert temperature (T) and relative humidity (RH) to a monthly average dew point temperature (T_D), we utilize the equation

$$T_D = \left(\frac{RH}{100}\right)^{\frac{1}{8}}(112 + 0.9T) + 0.1T - 112 \tag{12}$$

which is taken from Wanielista et al. (1997). T and RH for Aas and Skogmo are downloaded from the homepage of "Bioforsk", while received from SMHI for the Swedish stations. The most ideal is to use average values from 20-30 years. T_D is calculated for each month of the year, and then a monthly average over a time period of approximately 10 years is found for Aas and Skogmo. The Swedish stations have observations of temperature and relative humidity for many years, so for these stations the final dew point temperatures are based on an adequately number of years. Table 4 gives the averages of dew point temperature used to calculate the average amount of water vapour for each of the stations.

Table 4: Climatological averages of monthly dew point temperature ($°C$) for all the stations.

Station	J	F	M	A	M	J	J	A	S	O	N	D
Vaxjo	-3.3	-4.0	-3.4	-0.9	2.9	7.0	9.6	10.1	7.0	4.4	0.2	-2.4
Landvik	-4.5	-5.9	-2.0	0.9	4.0	7.1	12.0	11.1	8.3	4.4	0.9	-1.4
Norrkoping	-3.9	-4.6	-3.9	1.6	2.1	6.7	9.6	9.6	6.2	3.7	-0.3	-3.1
Karlstad	-4.4	-4.6	-3.2	-5.8	4.2	8.6	11.5	11.5	7.2	4.1	-0.3	-3.6
Aas	-3.7	-5.0	-3.6	1.3	5.0	8.4	12.2	11.7	7.9	3.7	0.1	-3.4
Bergen	-2.8	-3.3	0.6	2.4	3.0	6.0	10.8	10.3	9.1	4.8	2.0	-0.1
Kise	-8.9	-11.4	-4.7	-0.7	2.3	6.2	11.4	10.6	6.7	2.5	-1.4	-5.6
Fureneset	-3.3	-4.5	0.3	2.4	3.9	6.8	11.3	10.8	8.7	4.1	1.7	1.0
Ostersund	-9.2	-8.6	-7.5	-5.1	-0.7	3.9	7.3	7.0	3.4	0.0	-4.4	-7.6
Umeaa	-9.1	-8.6	-6.4	-3.6	0.6	5.9	9.8	9.2	5.2	1.0	-3.7	-7.7
Skogmo	-5.2	-5.8	-5.0	0.0	3.7	7.6	11.0	10.6	7.2	2.3	-1.7	-4.2

- Aerosol optical depth (τ):

  This parameter can be put in directly if available, or estimated from the precipitable water vapour amount (w) by using the equation

$$\tau_{0.5} = 0.1 + 0.05w \tag{13}$$

  where $\tau_{0.5}$ is the aerosol optical depth at 0.5 μm. Equation 13 is taken from Olseth & Skartveit (1989).

- Monthly regional albedo:

  Based on the location and climate of the observation stations and characteristic albedo values, the values of monthly regional albedo are divided into two groups. The first group is situated at the coast or at latitudes in the most southern part

of Scandinavia. These areas are less likely to have a snow-cover (especially a persistent snow-cover) and a highly reflective snow covering the ground for a long period. Members of the second group are further north, at higher elevations or at a location characterized by lower temperatures and away from the coast (often characterized as inland). Table 5 present the monthly values for the two groups.

Table 5: Climatological averages of monthly regional albedo for all the stations which is divided into two groups, depending on geographical location.

Group	J	F	M	A	M	J	J	A	S	O	N	D
1	0.25	0.25	0.20	0.15	0.15	0.15	0.15	0.15	0.15	0.15	0.15	0.20
2	0.30	0.30	0.25	0.20	0.15	0.15	0.15	0.15	0.15	0.15	0.20	0.25

Aas, Bergen, Fureneset, Karlstad, Landvik and Norrkoping constitute the first group, while Kise, Ostersund, Skogmo, Umeaa and Vaxjo constitute the second group with higher climatologically averages. The hillsides above the free horizon are set to have albedo equal the regional albedo and they are treated as sloping linearly from the actual horizon to the instrument.

- Monthly atmospheric ozone amount (cm NTP):

  The seasonal variations of atmospheric ozone for every 10 degree of latitude is originally given in a table by Iqbal (1983), but are adjusted for each of the stations in this thesis. Increased latitude corresponds to increased ozone amount. Table 6 contains the monthly average ozone amount for Bergen (approximately located at 60°N). The ozone amounts for stations located further north or south are only deviation ± 0.01 cm NTP from the Bergen values, respectively, so these are excluded from the table.

Table 6: Climatological averages of monthly ozone amounts (cm NTP) for the Norwegian station Bergen.

Station	J	F	M	A	M	J	J	A	S	O	N	D
Bergen	0.33	0.39	0.42	0.40	0.39	0.36	0.34	0.32	0.30	0.28	0.30	0.31

By running the model with the corresponding input values listed above, files with hourly, daily, monthly and accumulated irradiations for the entire period are produced. Global, direct and diffuse solar radiation are estimated in addition to solar elevation and solar azimuth angle. The units of the irradiance data are MJ/m^2, except for hourly irradiance data which is given as W/m^2.

3.2.2   Problems concerning the observed and modelled solar radiation

Potentially, there are several problems which need to be handled when basing a study on data from different sources. First, there are often missing or erroneous values. For data on an hourly basis, these are replaced by not a number (NaN) and omitted from further work. Daily values containing the corresponding NaN are also omitted, to prevent calculating an erroneous daily global radiation.

Leap years are also a problem which needs to be handled. Among the five years (1996-2000) which this study is based on, 1996 and 2000 contains February 29. The clear sky model does not produce data for these extra days, so they were simply deleted from the datasets.

The routines on naming each of the hourly observations are different from institute to institute. At the Norwegian stations, the stated hour represent the average global radiation from the subsequent hour. One exception is Bergen, where they are recording the global radiation in true solar time. Consequently the recorded hour includes 30 minutes before and 30 minutes after the stated hour. Sweden on the other hand, uses the mean global radiation from the hour before the stated hour. Luckily all these data are recorded in the same time zone, one hour east of the coordinated universal time (UTC + 1). See table 7 for information about time zones and which time interval was originally included in the hour names.

Table 7: Detailed information about the station data. Time zones and time standards which the data are recorded in (TST/LST) are given in the table. How the observed and modelled hours are defined is also given for the stations.

Station	Time Zone	Operate in	Observed hour	Modelled hour
Bergen	UTC + 1	TST	11:00 = 10:30 - 11:30	11:00 = 10:30 - 11:30
Landvik	UTC + 1	LST	11:00 = 11:00 - 12:00	11:00 = 11:00 - 12:00
Karlstad	UTC + 1	LST	11:00 = 10:00 - 11:00	11:00 = 10:00 - 11:00

In table 7, Landvik represent the Norwegian stations (Skogmo, Fureneset, Kise and Aas) and Karlstad represent the Swedish stations (Umeaa, Ostersund, Norrkoping and Vaxjo). As already mentioned in the subsections 3.1.1 and 3.1.2, respectively, LST means local standard time (which in this case is UTC+1) and TST means true solar time.

To obtain a good global radiation estimate, accurate input parameters are important. Monthly climatologically averages are used as input and should ideally be averaged over a relatively long period. This is not available for all the stations, where only a few years form the basis for the averages.

3.3   Satellite derived solar radiation

Satellite derived solar radiation for the years 1996-2000 is downloaded from the Satel-Light server (http://www.satel-light.com). Hourly and daily averages of global irradiances are obtained by weighting two and 48 half-hourly values, respectively. Compared to the ground truth data which is the mean hourly global radiation, the satellite estimates are derived from pictures taken of the surface of the Earth at a specific time. It is not directly an hourly mean value, but rather a mean of two picture estimated values. Because of this, the daily global radiation values are more likely to match the ground truth data.

The satellite measurements accomplished by the geostationary satellite Meteosat form the basis for the Satel-Light server. A geostationary satellite travels above equator, at a longitude of zero degree and at the same speed as earth rotates. This way the satellite will constantly overlook the same surface area. It sees approximately one half of the earth and measures the reflected radiation in three spectral bands:

- visible (0.5-0.9 μm)

- water vapour (5.7-7.1 μm)

- infrared (10.5-12.5 μm)

where images produced in the visible channel is used to produce the Satel-light data.

It takes approximately twenty-five minutes for Meteosat to get all pixels from the North Pole to the South Pole, and a picture is produces every thirty minutes. Because of this, the time these satellite pictures are produced will differ slightly from the actual time of measured reflection.

Meteosat images at the resolution 2500 * 2500 pixels are the basis for the Satel-Light data. The pixels representing Western and Central Europe (1280 pixels in longitude and 760 pixels in latitude) are processed, before the value in one pixel is averaged over three pixels in latitude and five pixels in longitude. This compensates for the variation the radiation can have during the half hour period, and gives the best match between satellite and measured solar radiation data.

By taking one over two pixels in latitude and longitude for a total of 640 pixels in longitude by 380 pixels in latitude, the image resolution is again reduced. The area a pixel now covers depends on how far north the site is localized. In North Africa a pixel represent a square of about five kilometres in longitude and six kilometres in latitude, while around Scandinavia a pixel represent a square of at about five kilometres in longitude and sixteen kilometres in latitude.

3.3.1   The Heliosat procedure

The Heliosat model gives surface global radiation from satellite measurements of the cloud cover. Despite being a simple model, it gives good results. The procedure was first presented in 1986 (Cano et al.), but has since been modified by others since then. The version described in this thesis was presented and used by the EU-project Satel-Light (www.satel-light.com).

The whole concept of deriving solar radiation from satellite pictures by using the Heliosat procedure, is based on the assumption that the albedo of a cloudy atmosphere is bigger than the albedo of the ocean and the surface of the earth. By applying this assumption, the first step in the process is to determine the cloud index (n):

$$n = \frac{\rho - \rho_g}{\rho_c - \rho_g} \tag{14}$$

where ρ is the actual albedo, ρ_g is the ground albedo and ρ_c is the cloud albedo. The ground albedo and the cloud albedo are calculated based on monthly values of the albedo under cloud free and totally cloudy conditions. The cloud free albedo has a daily and seasonal variation due to changes in the direction of incident sunlight and surface characteristics. The cloud index is a estimate of the cloud cover and varies normally between zero (a cloud free sky) and one (a cloudy sky), but it can reach values below and above these limits.

The relationship between the global clear sky index k_g and the cloud index n (given below) is found empirically from data prior to 1996 by the SATEL-LIGHT team (Fontoynont et al. 1998) and can be used in step two to obtain the surface global irradiance:

$$k_g = 1,20 \text{ for n} \leq -0,2 \tag{15a}$$

$$k_g = 1 - n \text{ for} - 0,2 \leq n \leq 0,8 \tag{15b}$$

$$k_g = \frac{(31 - 55n + 25n^2)}{15} \text{ for } 0,8 \leq n \leq 1,1 \tag{15c}$$

$$k_g = 0,05 \text{ for n} \geq 1,1 \tag{15d}$$

where the global clear sky index k_g is defined as the ratio between the actual global irradiance H_g (observed or satellite-derived) and an average cloud-free global irradiance H_0 (which is the sum of a direct and a diffuse component):

$$k_g = \frac{H_g}{H_0} = \frac{H_g}{H_{b0} + H_{d0}} \tag{16}$$

H_0 is the sum of cloud-free beam irradiance H_{b0} (Kasten (1996), Page (1996)) and cloud-free diffuse irradiance H_{d0} (Dumortier 1995).

There are both advantages and disadvantages with the Heliosat procedure. First, advantages:

- Heliosat is an simple model.

- Few input parameters.

- Gives data with an almost continuous spatial and temporal coverage. This is because the procedure is based on measurements from a geostationary satellite.

- Good precision.

Second, disadvantages:

- During situations with snow-cover it can be difficult to distinguish a cloud free sky from a cloudy sky.

- During situations with low sun elevation it can be difficult to distinguish a cloud free sky from a cloudy sky.

It is important to note that the satellite has no information about the horizon. A pyranometer receives direct solar radiation only during hours where the solar elevation exceeds the surrounding topography. Potentially, this would result in an overestimation of the global radiation at sites where mountains are blocking the direct component of the solar radiation for some extent of time.

As mentioned in the list of disadvantages with the Heliosat method, the satellite interprets reflections of solar radiation from snow-covered ground as reflection from clouds. This causes an underestimation of the surface global radiation, since the satellite consequently sees more clouds than it in reality is. This is not necessarily revealed from data on a daily basis, but is easily seen from hourly data. Actually, the effect of horizon and snow-covered ground might cancel each other out. The problems concerning snow-cover and horizon are examined further in section 4.2.2.

4   Results and discussion

4.1   Global radiation in Scandinavia

Hourly global radiation at eleven Scandinavian sites exists for the period 1996-2000. To control the quality of these data, they are tested against the output from a reliable method as described in Olseth et al. (1996). For each of the eleven stations, hourly clear sky global radiation was estimated by the McMaster model (see section 3.2 for information about the model). Daily measured global radiation and modelled clear sky global radiation are calculated from the measured and modelled hourly values.

4.1.1   Quality control of the global radiation

Global radiation, the sum of direct and diffuse radiation, are not necessarily measured by exactly the same instrument at each of the stations in this study. Instruments are also replaced by updated editions and this may in some cases cause differences in the data sets. A quality control is therefore necessary to assure comparability of the measurements from the different stations and for the whole period.

For the quality control, measured daily global radiation is compared to daily clear sky global radiation estimated by the McMaster model. For the latter, inputs are climatologically monthly averages and outputs are global irradiances. The model run require horizon panorama as an input parameter if this is available, otherwise it is run for an unobscured (free) horizon.

Figures 14 - 17 show measured daily global radiation for the years 1996-2000 for each station and the corresponding modelled daily clear sky global radiation. The clear sky curves are different from station to station, but are equal for the five year period for each station. As mentioned above, only climatologically monthly averages are used as model input, and hence there are discontinuities of the curves from one month to another. Thus, as the monthly average amount of precipitable water is increasing in the first half year there is a slight drop down in estimated clear sky irradiance from one month to the other. In the second half year there is a similar increase at the change of month.

As seen in figure 14 - 17, measured and modelled daily global radiation is high during summer and low during winter. The yearly variation largely depends on the solar elevation, which is considerable larger during summer than winter. The station locations varies in latitude ($56.93 - 64.51\,°$N) and has different altitudes (6-376 meters above sea level). These differences will in some degree result in variations in solar elevation and sunshine duration between stations, especially the difference in latitude. Mountains surrounding the locations are also important to consider.

The daily global radiation varies from day to day. It depends on the cloud amount and cloud type during the day. Normally the clouds block out the direct solar radiation, and
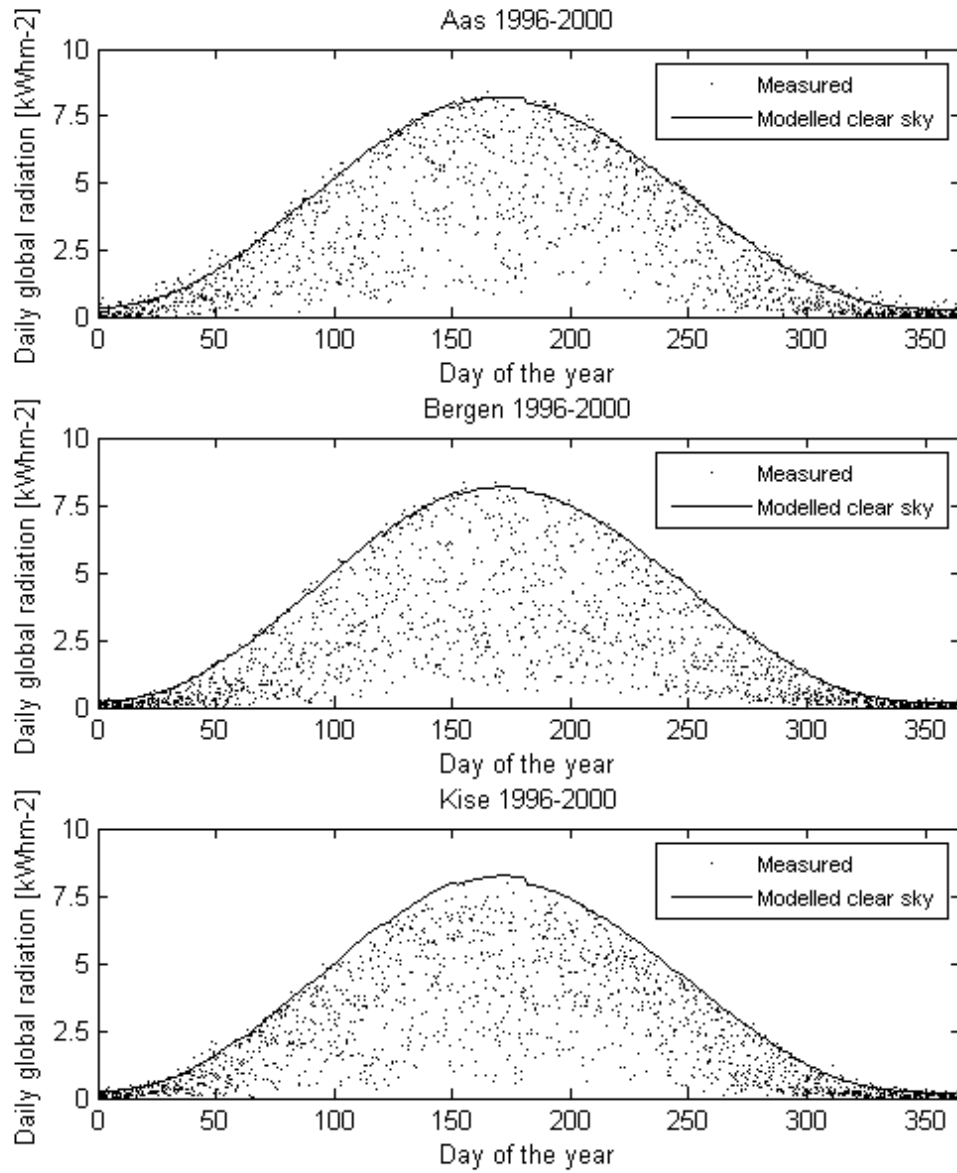
Figure 14: Measured daily global radiation (dots) and modelled daily clear sky radiation (fully drawn curves) for the three Norwegian stations Aas, Bergen and Kise for the years 1996-2000. The units are kWh/m^2.
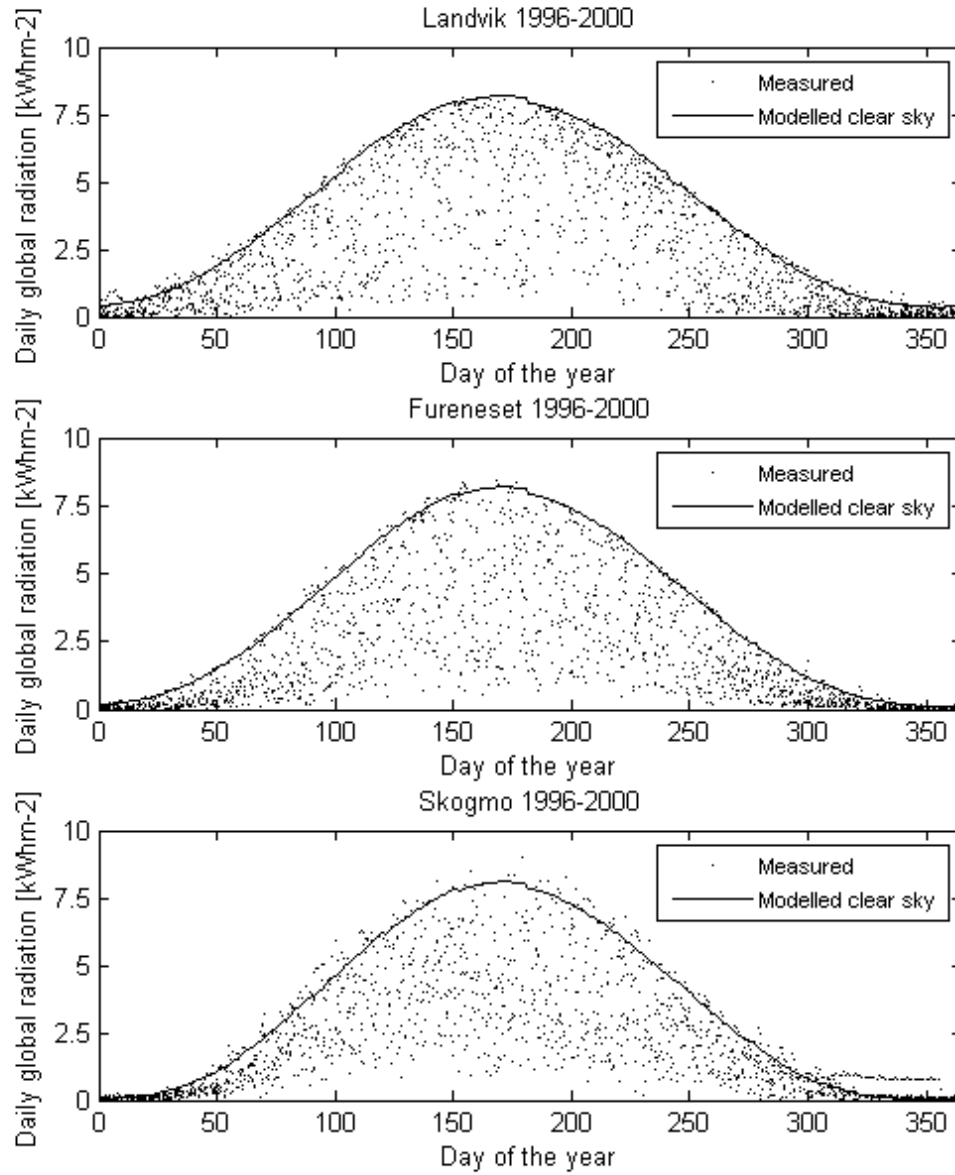
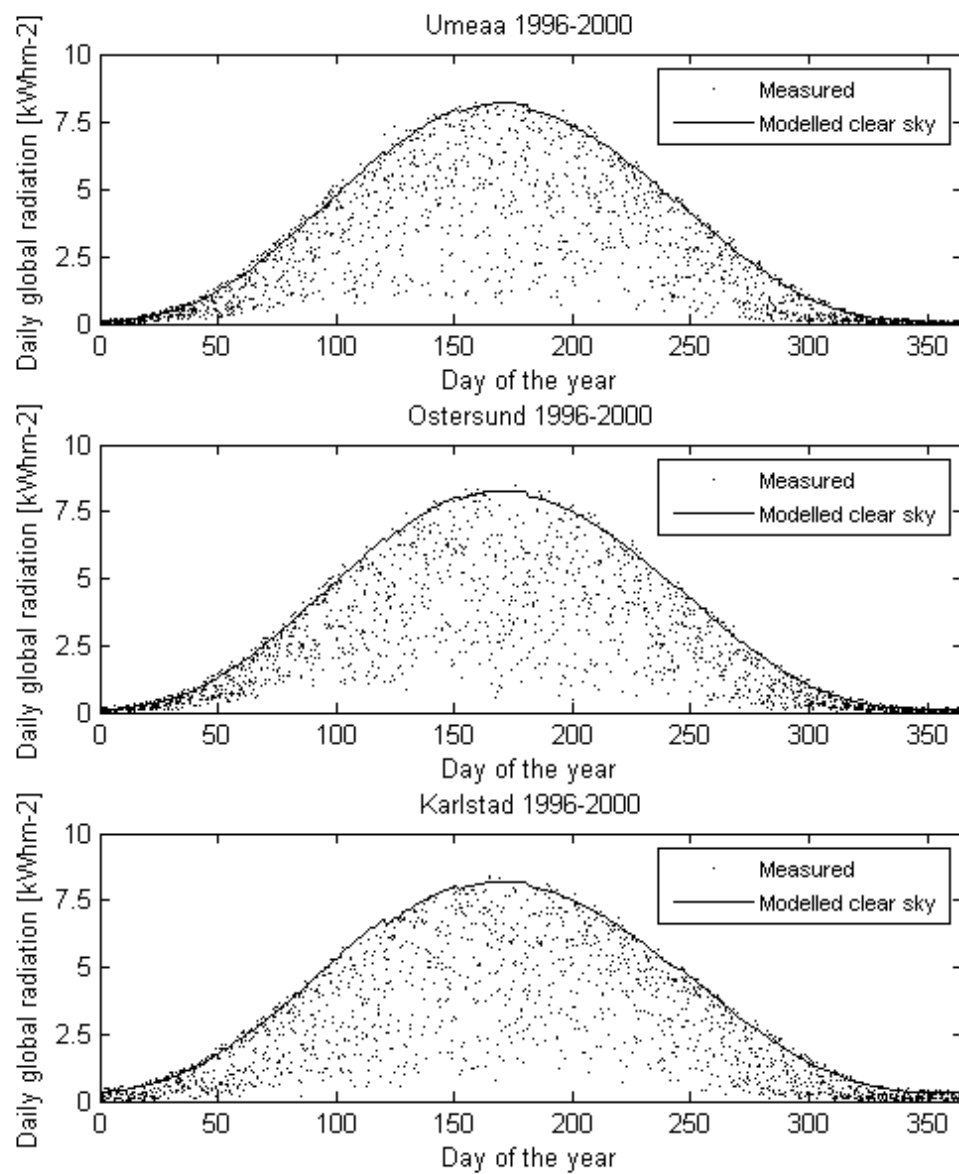Figure 15: Same as in figure 14, for the three Norwegian stations Landvik, Fureneset and Skogmo.

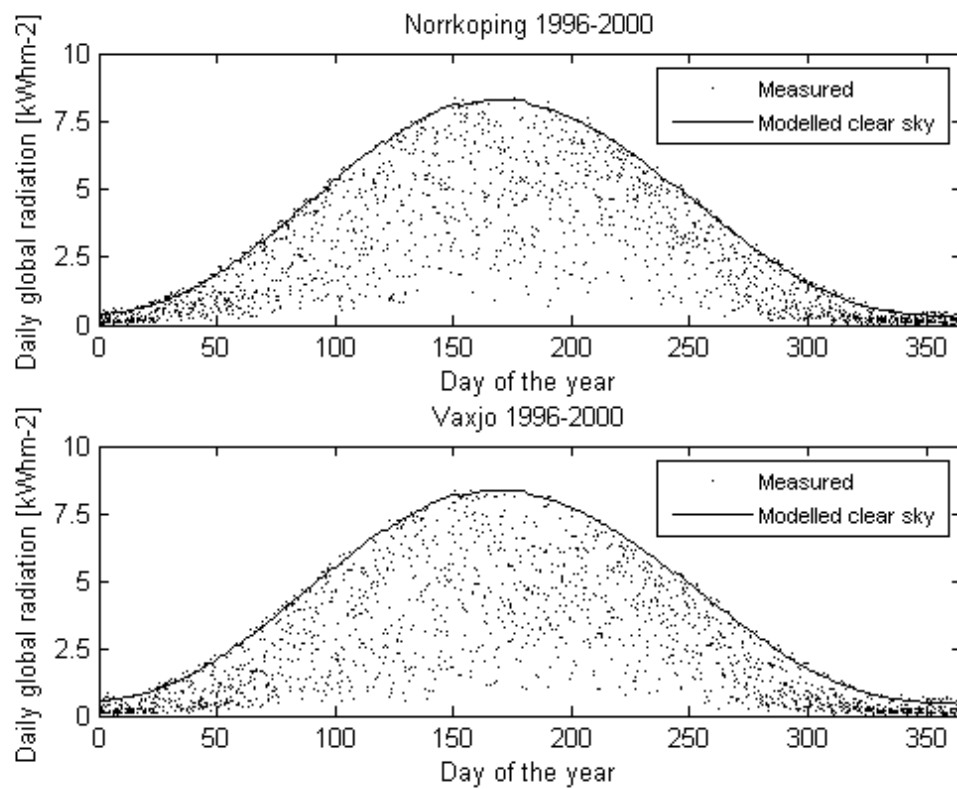Figure 16: Same as in figure 14, for the three Swedish stations Umeaa, Ostersund and Karlstad.

Figure 17: Same as in figure 14, for the two Swedish stations Norrkoping and Vaxjo.

causes a dramatic reduction of the global radiation. Despite a slightly increased diffuse radiation when certain cloud types are present, overcast situations have lower global radiation than clear sky situations. Cloudy situations are represented by values below the modelled clear sky curve in figures 14 - 17.

Clouds might also have the opposite effect. Values larger than the clear sky value are possible if the sun is not covered and when radiation is scattered into the direction of the instrument by clouds or even other atmospheric particles. Measured values above the clear sky curve are most likely special cases of radiation being scattered in the direction of the instrument or multi reflection from clouds. If snow is covering the surroundings of an instrument, this might also increase the amount of radiation reflected towards the instrument. Besides, as only monthly climatologically values are used as input to the clear sky model, the actual day-to-day variations of precipitable water are not taken into consideration.

Figure 14 shows that the modelled clear sky curve coincides with the highest observed values at Aas (top section) and Bergen (middle section), especially for the latter. It is a slight tendency of observations being of greater value than the clear sky curve at Aas, especially in winter. For Kise, the highest observed values do not coincide with the corresponding modelled clear sky values. The ground truth data are too low and will be inspected closer in figure 20, where the measured and modelled global radiation is given separately for each of the five years. This is also done for Aas and Bergen, but these are not included in the results.

For Landvik, figure 15 shows that the modelled clear sky curve coincides with the highest observed values. This corresponds well to the results from plotting the data year by year (not shown here). During the winter months, it is a slight tendency of observations exceeding the modelled clear sky radiation. Multi-reflection from clouds and reflection from snow-covered mountains can be the reason. For Fureneset and Skogmo, it is necessary to include the figures showing the global radiation for the five years separately, see figure 18 and 22 for further details.

As seen from figure 16, the modelled clear sky curve coincides with the highest observed values at Umeaa, Ostersund and Karlstad for the years 1996-2000. The clear sky curve is slightly underestimated periodically for the three stations, especially in the first two-three months but also towards the end of the year. The dew point temperature used as input is calculated from an equation where temperature and relative humidity are the required input parameters. The precipitable water estimated from this dew point temperature might be too high, which results in a clear sky curve too low for the season.

Ostersund and Karlstad are both situated inland and might experience more reflection from the surroundings than first assumed (too low albedo). Umeaa and Ostersund are also situated at relatively high latitudes where snow-cover is more likely to occur and persist. If this is not sufficiently accounted for, the clear sky curve might be estimated too low during winter. Information about snow-cover is not available for any of the Swedish stations in this thesis, so it is not possible to verify this against observations.

Overall, the modelled clear sky curve coincides with the highest observed global radiation values for all the years in Norrkoping and Vaxjo. As shown in figure 17, some ground truth values are slightly higher than the estimated clear sky curve for these two stations also. This is not the case during summer months. Possible explanations are multiple reflection from clouds and reflection from snow-covered mountains, or too high input values of precipitable water or even a combination.

Figures 14 - 17 show the results of a quality control of the measured daily global radiation and modelled daily clear sky radiation for all the eleven stations. In addition to controlling the quality of the data for the whole five year period, it has been done for each year separately. The latter reveal some problems in the measurements at three of the stations, and are presented below (the others are as already mentioned, omitted).

Fureneset

Measured daily global radiation and the modelled daily clear sky curve for Fureneset are shown year by year in figure 18. In the first two and a half month of 1997 there are large negative values. As shown in figure 19, they are especially large during night. This might also be the case during daytime, only here they are hidden by larger positive values. Errors like this in the measured data are either caused by erroneous cable or instrument conditions. During the summer of 1997, some measured global radiation values are higher than the modelled clear sky curve. This is the first summer after the period with large negative values, so the outliers might have something to do with the same instrument error. Other that this, the clear sky curve coincides well with the highest measured daily values for all the years.

Kise

Figure 20 shows that for Kise the highest observed values coincide with the estimated clear sky curve for the years 1999-2000. For the period 1996-1998 the highest observations lies below the modelled clear sky curve. As noted in section 3.1.1, the CM1 pyranometer was replaced by a CM11 pyranometer on 18 August 1998. The first instrument has lower maximum values, and can explain why the measured values do not coincide with the modelled clear sky curve. Except for some observations above the clear sky curve during wintertime in 1999 and 2000, which might be explained by multiple-reflection from clouds and reflection from hillsides covered with snow, the last two years looks good. Data from the period 1996-1998 are of poor quality and will be discarded for further work with satellite derived global radiation (see also figure 21).

As seen from figure 21, the two periods have different relative frequency distributions of the clear sky index. The period 1999-2000 has more approximately clear days, which coincides with the results from figure 20. The fraction of low clear sky indices is larger in the right section than in the left section. This combined with a large relative frequency of clear sky indices close to one in 1996-1998, results in average clear sky indices equal to 0.603 and 0.580 for 1996-1998 and 1999-2000, respectively. The results revealed in figure 21, would not necessarily have been discovered if omitting the quality control.
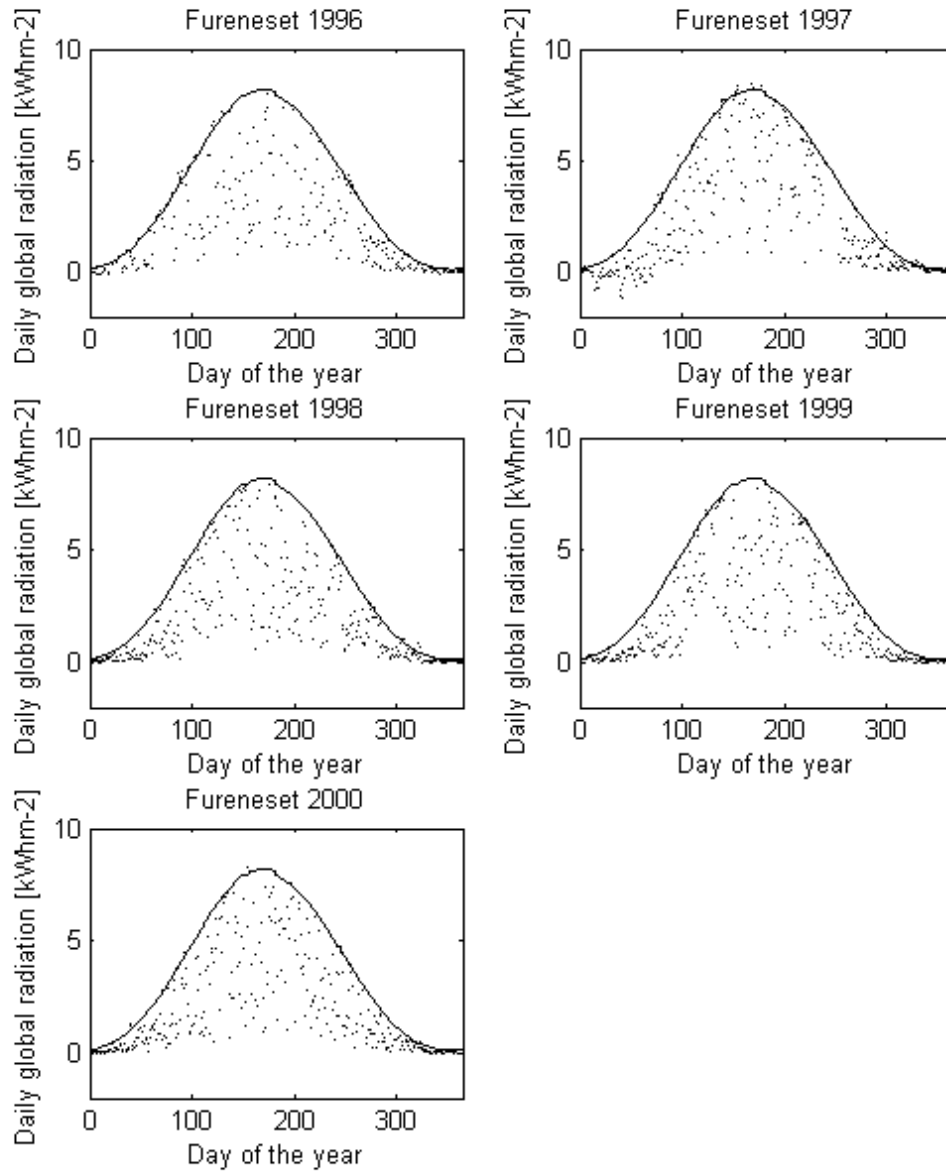
Figure 18: Daily measured global radiation (dots) and modelled daily clear sky radiation (fully drawn curve) for the Norwegian station Fureneset for each of the years 1996-2000. The units are $kWhm^{-2}$. Note that the axis is different from the axis in figures 14 to 17.
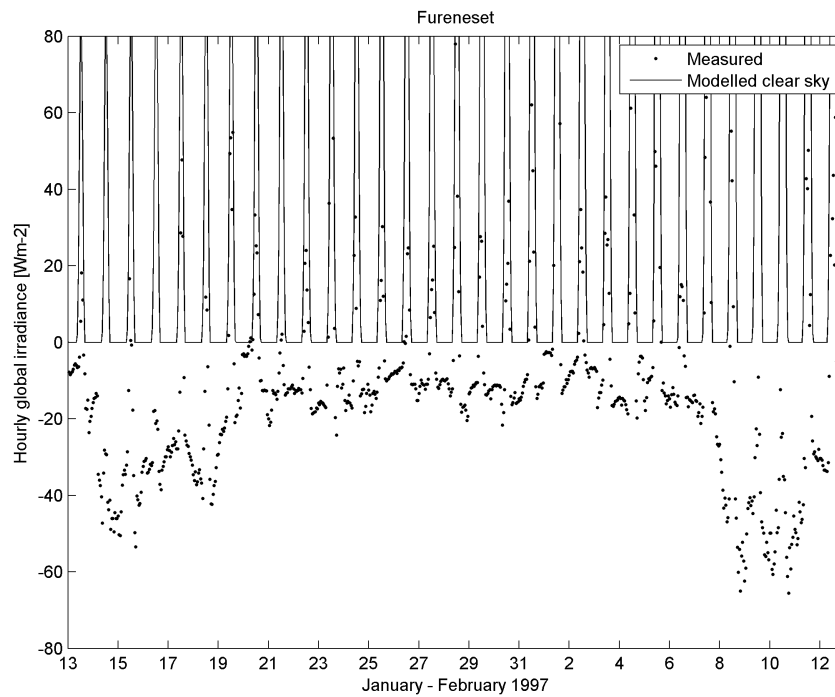
Figure 19: Observed (dots) and modelled (fully drawn curve) hourly global radiation for Fureneset during the second part of January and the first part of February 1997. The units are Wm^{-2}.
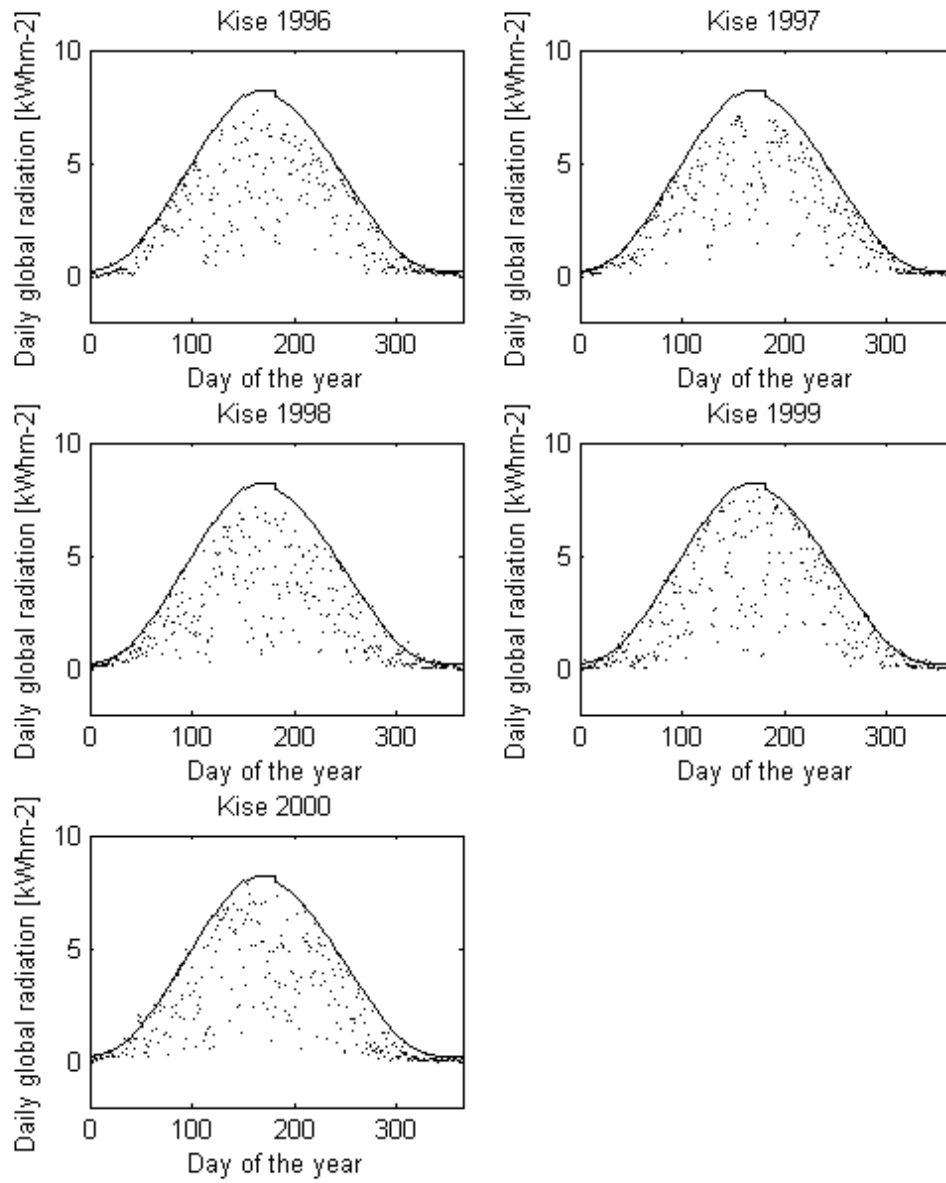
Figure 20: Same as in figure 18, for the Norwegian station Kise.
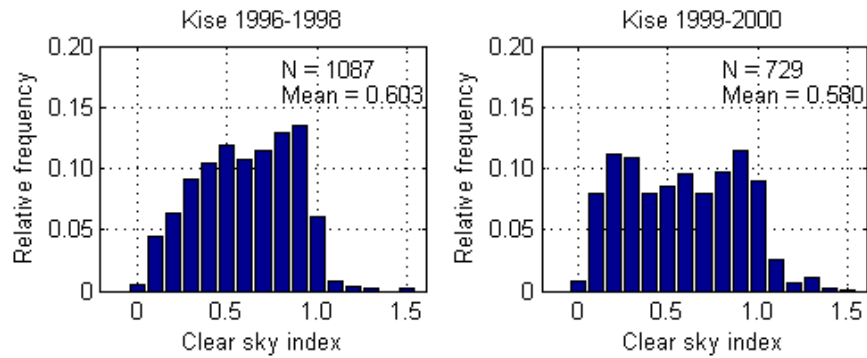
Figure 21: The relative frequency distribution of daily ratios between measured global radiation and modelled global clear sky radiation (clear sky index) for the Norwegian station Kise. The left section represent the period 1996-1998 and the right section represent 1999-2000. The number of days plotted (N) and the corresponding mean values are shown in the respective plots.

Skogmo

As seen from figure 22, the clear sky curve does not coincide with the highest measured daily global radiation values at the Norwegian station Skogmo. Periodically, daily values lies above the modelled clear sky curve. Some values lies right above the clear sky curve, while other lies beyond the modelled value. This is also the case during winter months for the last two years, when approximately all the values lie above the clear sky curve. The latter might be explained by the replacement of the measuring instrument in July 1998. After the installation of the new instrument, it was recording larger negative values during the nights. Bioforsk compensated for this on 29 October 1998, by lifting the offset $30\,\mathrm{Wm}^{-2}$. Observed daily global radiation values larger than the modelled clear sky curve, suggests that the accomplished compensation might be slightly too large.

In addition to outliers and a too high offset, something is happening in the end of 1997. On the 21 December 1997, the measurements goes from being larger than the modelled clear sky values to a sudden drop before the clear sky values stabilize at approximately the modelled value. The measured and modelled global radiation for this period is presented on an hourly basis in figure 23. Bioforsk do not have records of instrument replacements and comprehensive maintenance older than 1998, so an explanation of this other than an instrument error can not be found.
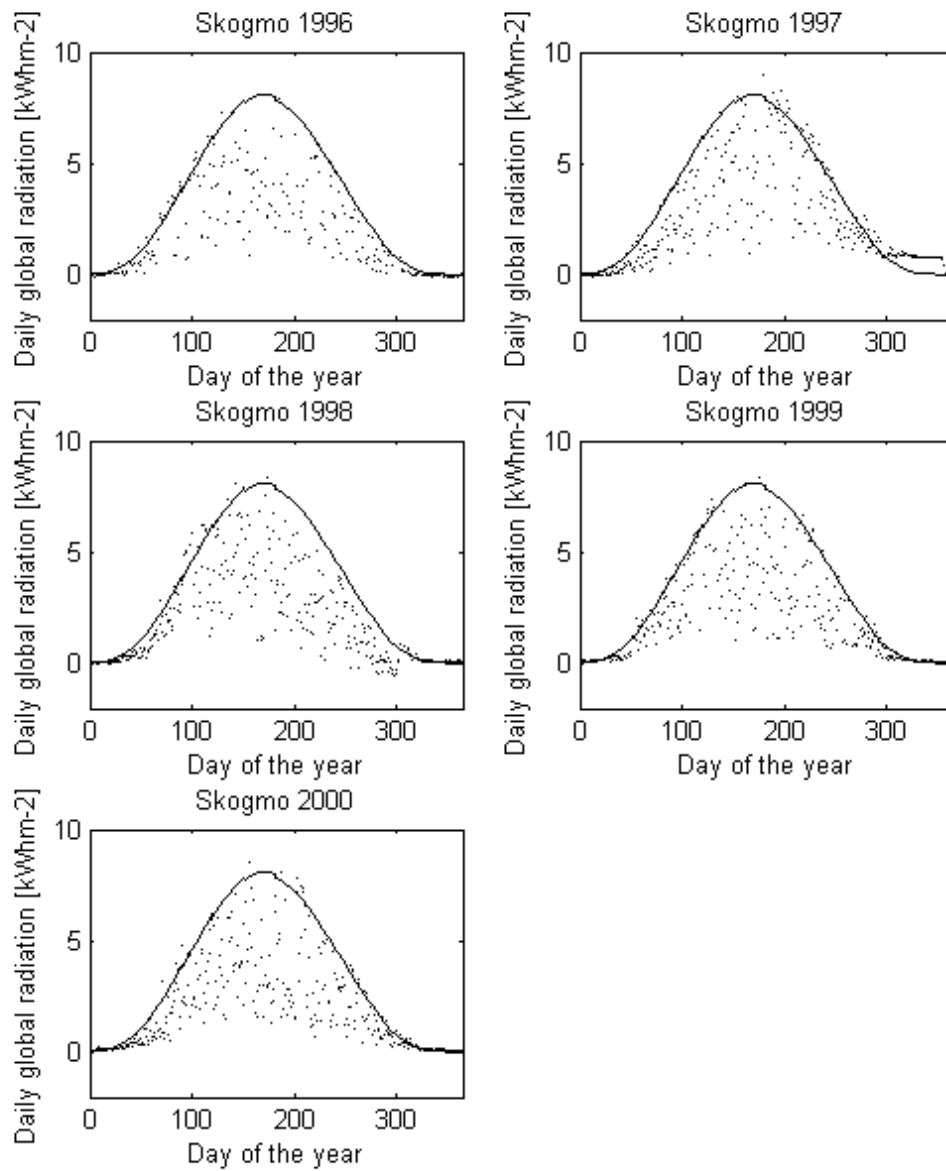
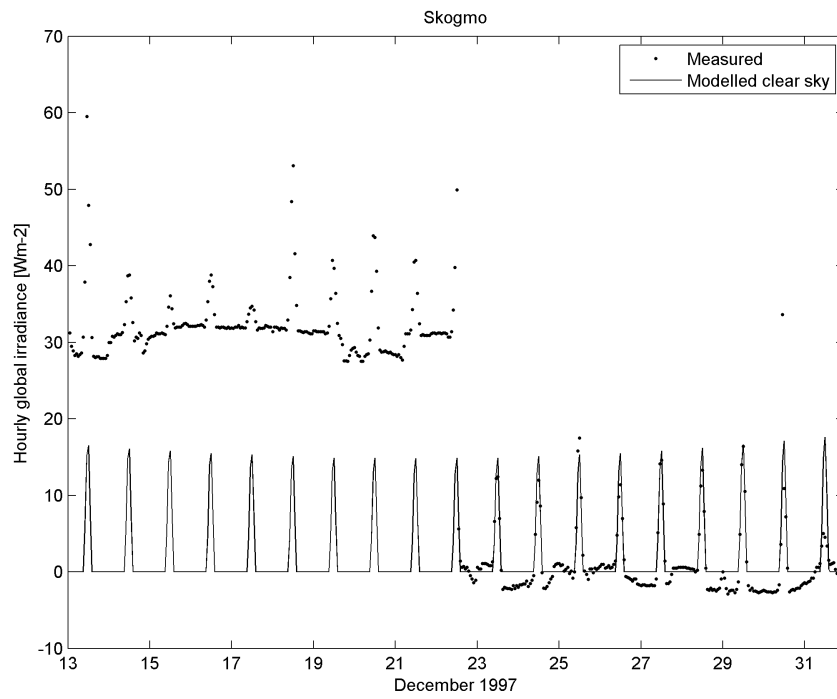Figure 22: Same as in figure 18, for the Norwegian station Skogmo.

Figure 23: Same as figure 19, for Skogmo and the second part of December 1997. Note that the axis is different from the axis in figure 19.

4.1.2   Relative frequency distribution of the clear sky index

The ratios of daily measured and modelled clear sky global radiation, also called daily clear sky indices, are produced for the years 1996-2000 (for the years 1998-2000 for Fureneset and for the years 1999-2000 for Kise). This is done for all the stations in figure 24 and 25, except for the Norwegian station Skogmo. The clear sky indices are divided into groups of width 0.1, where overcast days have a low clear sky index and clear days have clear sky index close to one. Values in between represent partly cloudy days with a combination of a changing cloud amount. Clear sky indices larger than the clear sky value might be caused by multiple scattering or reflection from clouds and snow-cover, inaccurate input-data to the clear sky model or measuring errors. To be able to present and compare the results of the relative frequency distributions for the different stations, clear sky indices larger than 1.5 are set to be equal 1.5.

The right section of figure 24, shows the relative frequency distribution of daily ratios between measured global radiation and modelled clear sky global radiation for the Norwegian stations Fureneset (1998-2000) and Bergen (1996-2000). The distribution of clear sky indices is rather similar and shows a large relative frequency of low clear sky indices. Fureneset and Bergen have the lowest average daily ratios with 0.503 and 0.545, respectively. The average daily ratio for the period 1998-2000 at Bergen is 0.517, which is lower than the corresponding value for the period 1996-2000 (0.545) and closer to the value at Fureneset for 1998-2000. These clear sky indices indicate that Fureneset and Bergen have approximately the same large fraction of cloudy days. Both stations are located on the west coast of Norway, with Fureneset further north than Bergen. Low pressure systems coming in from west with humid air are typically hitting the Norwegian coast at these latitudes. Air masses pushed aloft by topography increases the cloud amount, often combined with precipitation. This results in less clear days than locations east of the Scandinavian mountains covering the central parts of Norway (on an east-west axis). In addition, both the west coast stations have a clear sky peak around one.

Aas and Landvik have a higher frequency of clear sky indices around one, compared to the clear sky peaks at Fureneset and Bergen. As seen from figure 24, Landvik generally has a larger fraction of clear sky indices close to zero than Aas. Clear sky indices above one are the case for Aas and Landvik, but the former also has a small fraction of values below zero. This results in average daily ratios of 0.616 and 0.599 for Aas and Landvik, respectively. According to the average daily ratios, Aas and Landvik have least clouds of the five Norwegian stations.

Figure 20 showed that the three first years of measured daily global radiation at Kise were deviating from the last two years. The frequency distribution of the clear sky index is presented for the two periods separately in figure 21, but only the results from the two last years are included in figure 24. According to the mean clear sky indices at the stations east of the Scandinavian mountains for the period 1999-2000, Aas has most clear days (0.618) followed by Landvik (0.583) and Kise (0.580). It is important to note that the differences between these stations are small and that the effect of excluding the
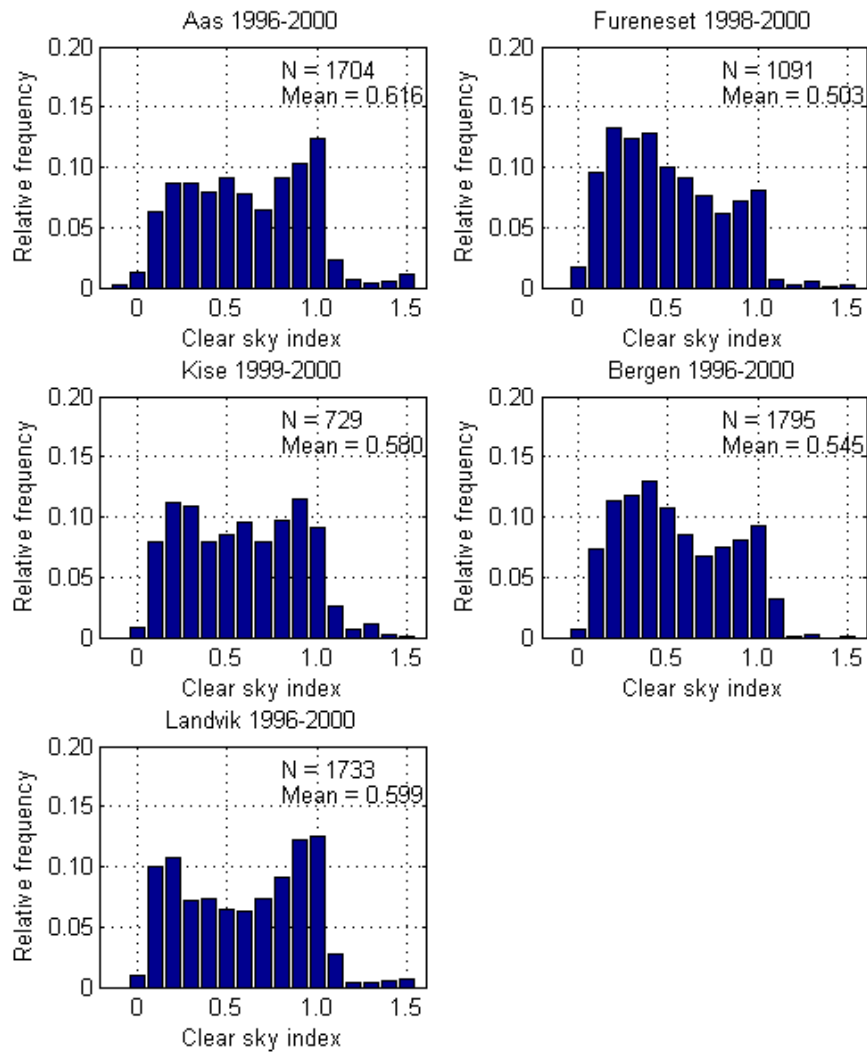
Figure 24: The relative frequency distribution of daily ratios between measured and modelled clear sky global radiation (clear sky index) for Aas, Landvik and Bergen for the five years 1996-2000. Fureneset and Kise are also included, but only for the period 1998-2000 and the period 199-2000, respectively. The number of days plotted (N) and corresponding mean values are shown in the respective plots.

three first years from the basis of the average is minor.

The relative frequency distribution of daily ratio between measured global radiation and modelled clear sky global radiation for the Swedish stations are shown in figure 25. The distribution of clear sky indices is most characteristic for Vaxjo which has a clear shift towards low values. A peak at 0.2, which is almost reaching a relative frequency of 0.15, is followed by a decreasing ratio with increasing clear sky index. This results in an average daily ratio for Vaxjo at 0.554, which is lower than for the other Swedish stations.

Karlstad and Norrkoping (shown in the two top sections of figure 25) have a rather similar relative frequency distribution of clear sky indices for the five years 1996-2000. Generally, these stations have a large fraction of clear days. Karlstad has slightly more clear days with an average clear sky index equal to 0.631 compared to Norrkoping with 0.619.

Of all the Swedish stations, Ostersund and Umeaa have the largest average daily clear sky index (0.689 and 0.691, respectively). This corresponds well with the frequency distribution in figure 25, where the frequency of daily ratios are increasing with increasing clear sky index. There is a shift towards large clear sky values combined with a large fraction of values above one for both Ostersund and Umeaa. As seen from figure 26 and 27, where the relative frequency distribution is presented for the summer and winter months separately, the clear sky indices above one are clear sky indices in winter situations.
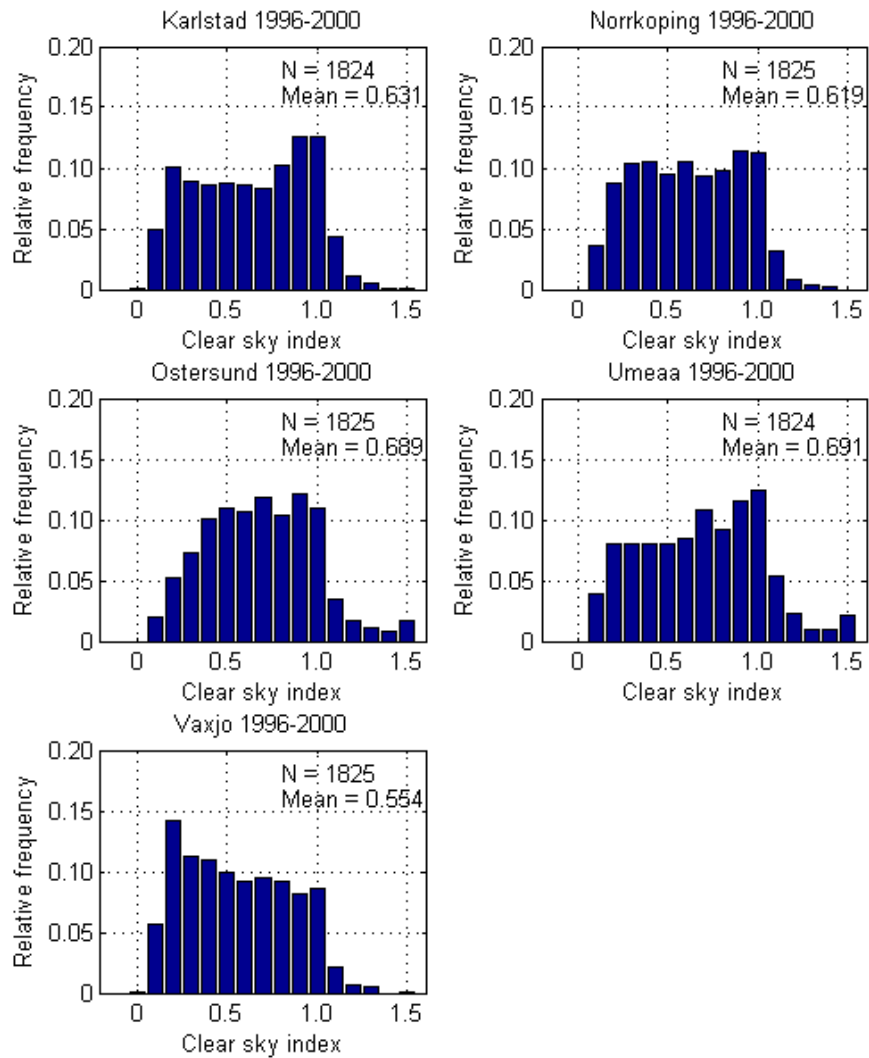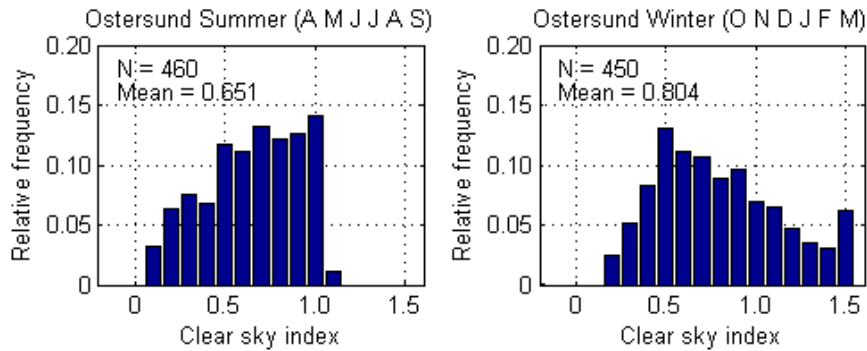
Figure 25: The relative frequency distribution of daily ratios between measured global radiation and modelled global clear sky radiation (clear sky index) for Karlstad, Norrkoping, Ostersund, Umeaa and Vaxjo for the five years 1996-2000. The number of days plotted (N) and corresponding mean values are shown in the respective plots.

Figure 26: The relative frequency distribution of daily ratios between measured global radiation and modelled global clear sky radiation (clear sky index) for Ostersund for the five years 1996-2000. Summer months (April-September) are given in the left section and winter months (October-March) are given in the right section. The number of days plotted (N) and corresponding mean values are shown in the respective plots.
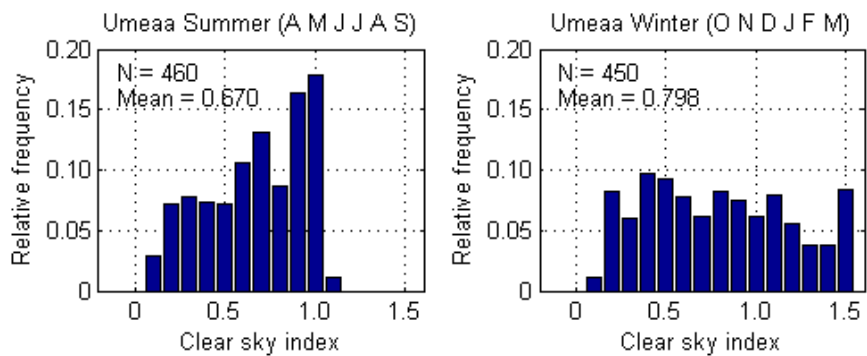

Figure 27: Same as figure 26, for Umeaa.

The solar elevation dependency of the hourly clear sky index at Umeaa is presented in figure 28, where only the summer months July - September are included. For low solar elevation (approximately $< 10°$), there are a larger fraction of clear sky indices above one. The global radiation values are small at low solar elevation, and the ratio of two small values can result in large clear sky indices. At larger solar elevations (approximately $> 15°$), the highest clear sky indices are roughly localized near one.
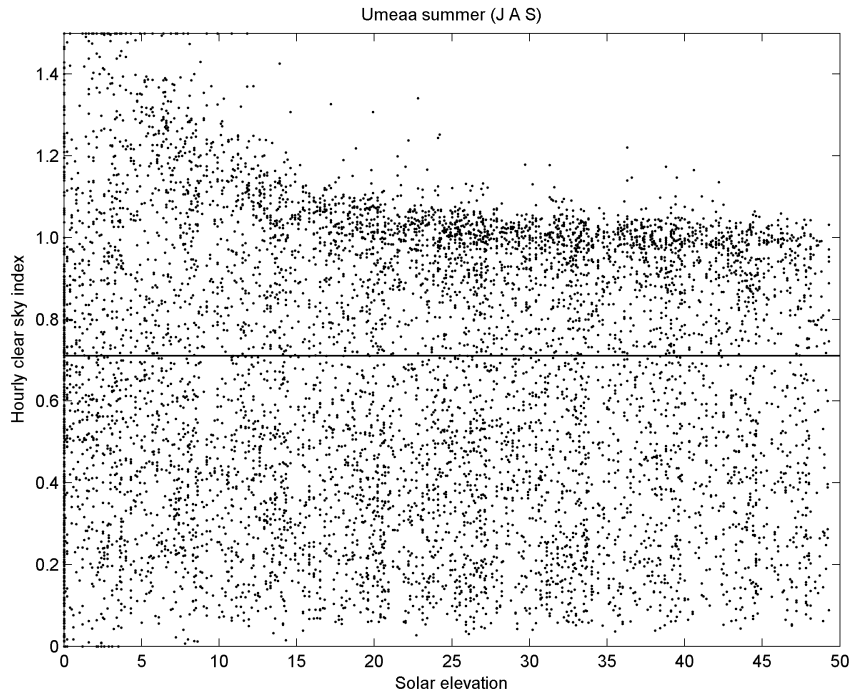

Figure 28: The hourly clear sky index for summer months (July - September) during the period 1996-2000 at the Swedish station Umeaa is given for all the modelled solar elevations. The average clear sky index is indicated by the horizontal line and is equal to 0.711.

Umeaa (0.688) and Ostersund (0.687) are the two stations with most clear days if the stations are ranked according to the relative frequency of clear days by comparing their average clear sky index. This is also the case when considering the frequency distribution for the seasons separately, with 0.651 and 0.670 during summer at Ostersund and Umeaa, respectively. Fureneset and Bergen have least clear days, where the average clear sky indices for the period 1998-2000 are 0.503 and 0.517. In general, the Swedish stations included in this study have a larger average clear sky index than the Norwegian stations, except from Vaxjo with a mean clear sky index approximately equal to 0.554.

4.2   Satellite derived global radiation

Observed daily global radiation at Landvik, Bergen and Aas are plotted against their Meteosat counterparts for the years 1996-2000 (figure 29). The same is done for Kise (1999-2000) and Fureneset (1998-2000), but only for two and three years, respectively. Figure 30 shows the results from plotting satellite derived global radiation against ground truth data for the five Swedish stations (1996-2000) Karlstad, Norrkoping, Ostersund, Umeaa and Vaxjo.

The daily average ground truth data and the daily average satellite derived global radiation is calculated for each station, and printed on the respective axes in figures 29 and 30. These values are given as OBS and SAT in table 8, respectively. Daily mean values in the figures have the unit kWh/m^2, while the corresponding values in the table has the unit Wh/m^2. The number of days forming the basis for the average values is given as N, and varies from approximately two to five years.

As shown in figure 29 and 30, the satellite slightly overestimates the daily surface global radiation. This is the case for all stations except from Aas, where the ground truth values are approximately equal or slightly underestimated. The latter is revealed in figure 29 if more decimals are included in the average global radiation values and in table 8.

By comparing the daily average observed and satellite derived global radiation, only minor differences are identified. In table 8, OBS varies from being approximately 2100 Wh/m^2 at Fureneset in Norway to 2650 Wh/m^2 at Norrkoping in Sweden. SAT varies from being approximately 2200 Wh/m^2 at Fureneset to 2750 Wh/m^2 at Vaxjo in Sweden. Overall OBS and SAT are approximately 2435 Wh/m^2 and 2525 Wh/m^2, respectively.

Table 8: Daily average ground truth (OBS) and satellite derived global radiation (SAT) for ten Scandinavian stations. Mean-bias-deviation and root-mean-square-deviation are given as MBD and RMSD, respectively, and have the unit %. The daily averages have the unit Wh/m^2. The number of days forming the basis for the averages is given as N.

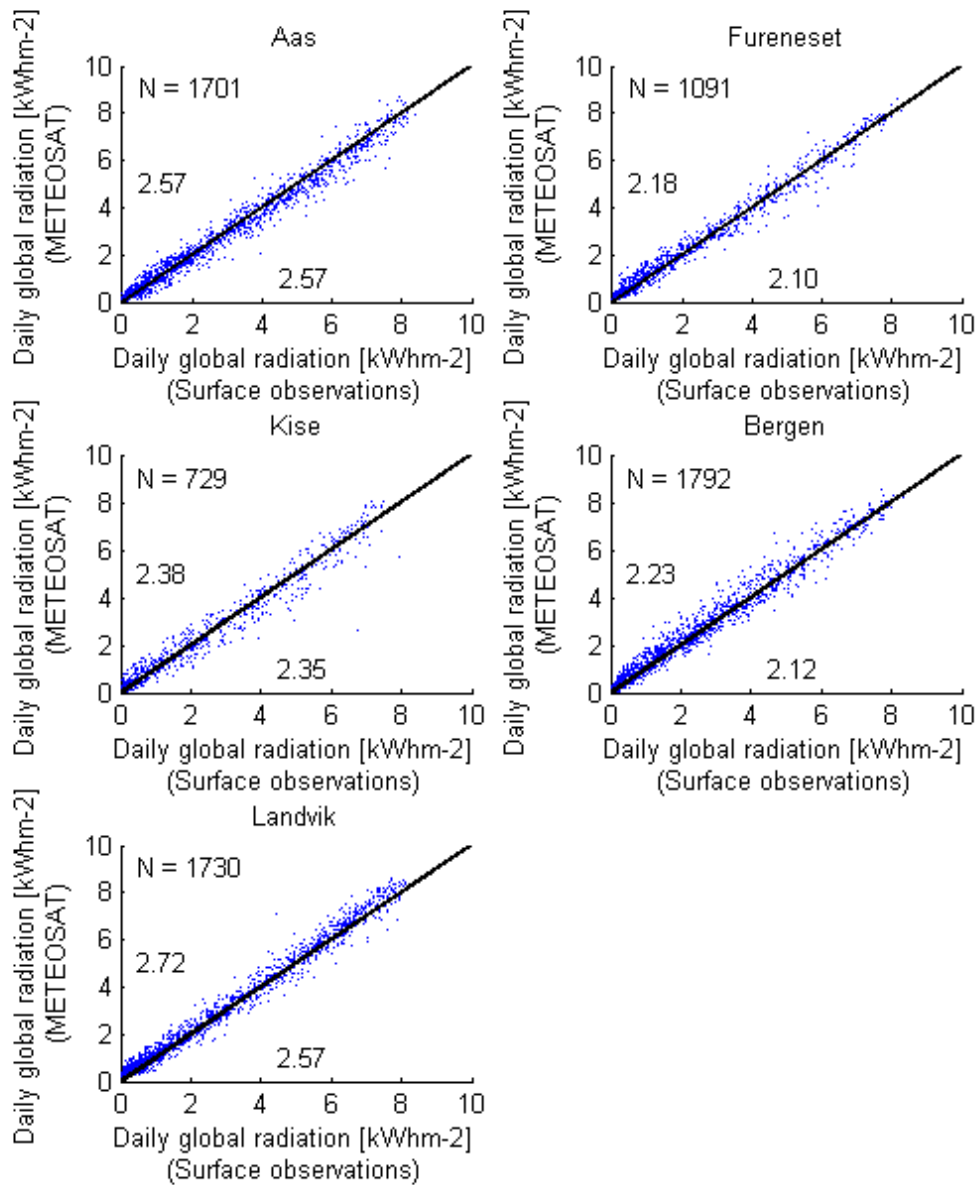| Station	N	OBS $[Wh/m^2]$	SAT $[Wh/m^2]$	MBD [%]	RMSD [%]
Vaxjo	1822	2514.0	2738.8	8.8	16.2
Landvik	1730	2566.8	2721.1	5.4	12.8
Norrkoping	1822	2636.1	2709.5	2.7	12.6
Karlstad	1821	2632.2	2668.6	1.2	12.4
Aas	1701	2571.1	2567.2	-0.8	13.1
Bergen	1792	2116.2	2231.0	5.6	16.6
Kise	729	2348.5	2376.4	1.1	19.0
Fureneset	1091	2094.9	2176.5	3.8	15.0
Ostersund	1822	2428.5	2498.8	2.8	17.9
Umeaa	1821	2440.5	2566.1	5.0	16.7

Figure 29: Daily global radiation derived by the Heliosat procedure from Meteosat data, plotted versus their ground truth counterparts at the five Norwegian stations Aas, Fureneset, Kise, Bergen and Landvik. Data from the whole period (1996-2000) are plotted, except for Kise (1999-2000) and Fureneset (1998-2000). The units are kWh/m^2. The 1:1 line is indicated, the number of days given as N and the average values (also given in kWh/m^2) printed on the respective axes.
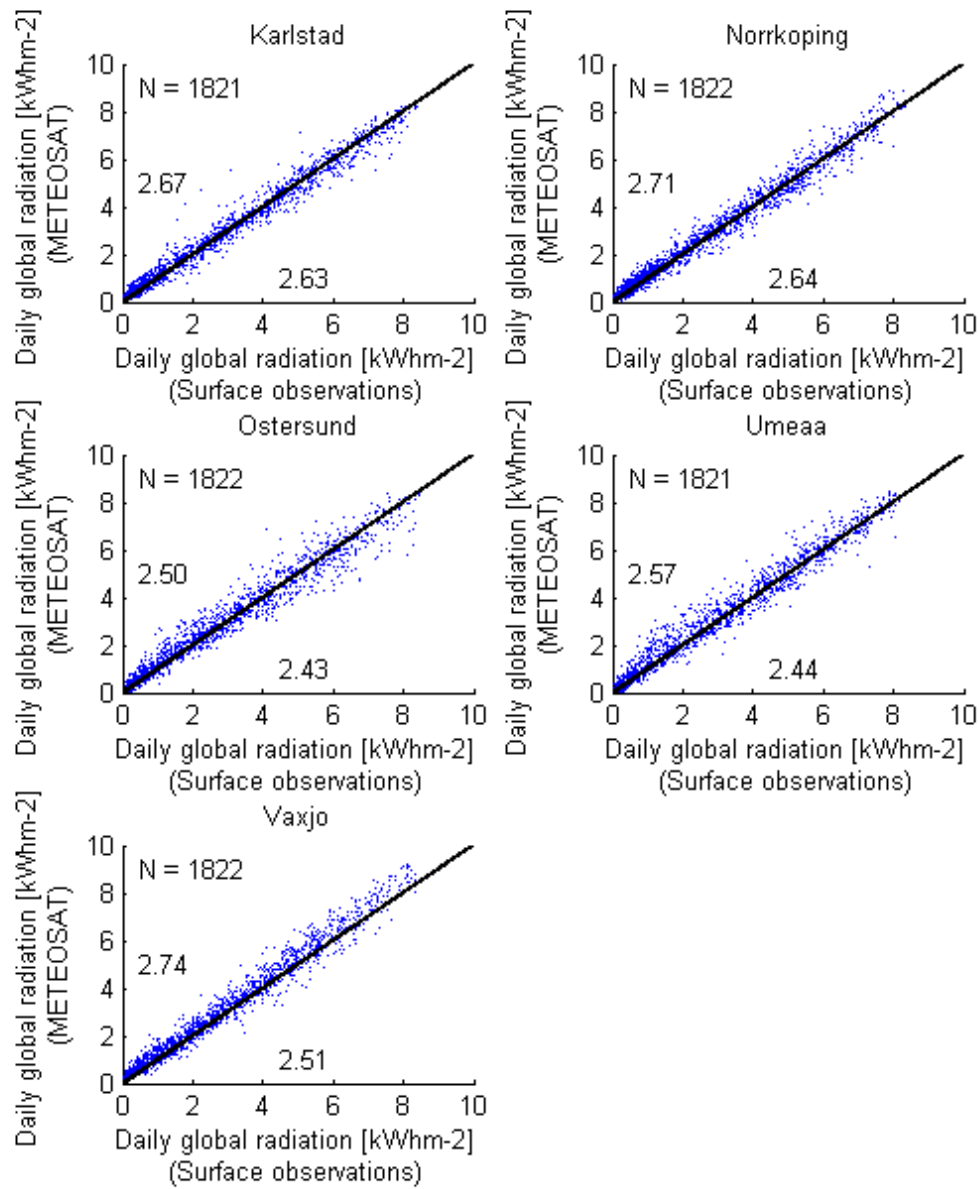
Figure 30: Same as figure 29, for the five Swedish stations Karlstad, Norrkoping, Ostersund, Umeaa and Vaxjo. Data from the whole period (1996-2000) are plotted.

Mean-bias-deviation (MBD) and root-mean-square-deviation (RMSD) of the difference between satellite derived global radiation and ground truth data are given in table 8 (see the first Appendix for information about the statistics). According to the MBD, the satellite overestimates the surface global radiation at all stations except from Aas. The MBD varies from being slightly negative at Aas (approximately -1%) to approximately 9% at Vaxjo. Aas is the station where the satellite estimate in average deviates least from the ground truth value. Kise and Karlstad are following Aas as the stations with best agreement, with approximately 1%. Umeaa (5%), Landvik (5%), Bergen (6%) and Vaxjo have MBD equal to or larger than 5%.

The RMSD in table 8, ranges from approximately 12 % at Karlstad to 19 % at Kise, with an average value of approximately 15% for all stations.

It is important to note that daily global radiation values are plotted in figure 29 and 30. Daily ground truth values are accumulated solar radiation received by the instrument measuring global radiation during one day and are more likely to match the corresponding satellite derived estimate. For the accumulated daily value, one overestimated hourly value might be compensated for by a following underestimated value. Estimated hourly values are compared on an hourly basis, and might deviate more from the ground truth data and thus be more scattered around the 1:1 line.

As an example, the scattering of hourly global irradiances derived by the Heliosat procedure from Meteosat data and corresponding ground truth data for Bergen (for the period 1996-2000) are shown in figure 31. Data are plotted for three solar elevation intervals, where solar elevations above 30° are shown in the top section. Solar elevations between 15° and 30° are shown in the middle section, while solar elevations between 0° and 15° and are presented in the bottom section.

Figure 31 shows that global radiation are more scattered around the 1:1 line when considering data on an hourly basis, compared to the results from plotting daily values in figure 29 for Norwegian stations and figure 30 for Swedish stations. For low hourly global irradiances, Heliosat slightly overestimates ground truth values at Bergen. High irradiances on the other hand, are slightly underestimated. These results would not be revealed if averaging over all solar elevations. Low mean hourly irradiances at all solar elevations indicate that a huge fraction of values are small.
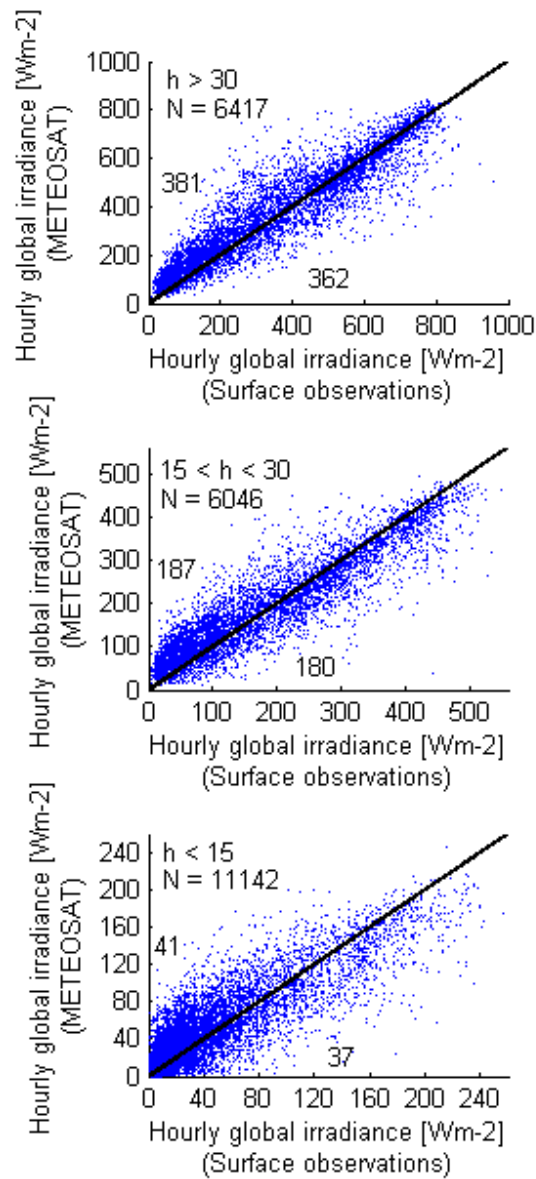
Figure 31: Hourly global irradiances derived by the Heliosat procedure from Meteosat data, plotted versus their ground truth counterparts within three solar elevation intervals (h in degrees) in Bergen during the period 1996-2000. The units are Wh/m^2. The 1:1 line is indicated and the number of hours plotted for each interval is given as N. The average values (also given in Wh/m^2) are printed on the respective axes. Note that the y-axes are different.

4.2.1 The relative frequency distribution of the satellite-observation difference

An additional way of visualizing the results from comparing satellite derived global radiation and ground truth data for all the stations with approved data quality, is obtained by presenting the frequency distribution of the actual and the relative difference between the satellite derived and observed values. By dividing the actual difference of the observed value, the relative difference is calculated. Both differences are calculated for all the stations (except Skogmo). In addition to presenting the frequency distribution for the whole period (top sections), the seasons are also presented separately (winter in the middle section and summer in the bottom section). Months between April and September are treated as summer and months between October and March are treated as winter. This monthly division is used for all stations, but it is not necessarily correct for all the locations. Winter might be longer for stations at high latitudes and summer might be longer for stations at low latitudes.

For Bergen, actual and relative differences are given in figures 32 and 33. According to figure 32, the distribution of actual differences is narrower in the winter than in the summer season, simply because the global radiation values are lower in winter. For relative differences (figure 33), winter has a less narrow distribution than summer. As the percentage difference between small values can be very high, there is also a distinct tail in the distribution, towards high positive relative differences. In the following, it will be focused on the relative differences.

In figures 33 - 42, the frequency distribution of relative differences are given for ten stations. In each figure, the groups of relative differences are of the width 0.1. Values larger or less than 1.4 and -1.4, respectively, are replaced by 1.4 and -1.4 and included in their groups. Days where the global radiation derived from Meteosat data are close to or equal the ground truth data are represented by the peak at zero in the frequency distribution of the satellite-observation difference. Positive values are equal to days where the satellite overestimates the surface global radiation, while negative values represent days where the satellite underestimates the surface global radiation. Average and median values are plotted in the respective figures.

Figures 33 - 42 show that for summer months, there is a larger fraction of days with satellite derived estimates close to the ground truth value, i.e. for all the stations the distribution of relative differences is narrower in summer months than in winter months. During summer, the mean relative differences are positive and less than 0.13 for all stations. In addition, the differences between mean and median values are small during summer.

Besides having a less narrow distribution, the winter months have a high number of large values. All stations except Karlstad, Norrkoping and Ostersund have between 10 and 20 % of the relative differences above 1.35. During this season the median values are thus closer to zero than the mean values. As examples, for Fureneset (figure 34) and Kise

(figure 35), between 15 and 20 % of the days have relative differences above 1.35 during winter. The mean (and the median) relative differences are 1.49 (0.32) for Fureneset and 0.82 (0.20) for Kise.

According to figures 33 - 42, the best agreement between satellite derived and ground based daily global radiation appears for the Swedish stations Karlstad (figure 36) and Norrkoping (figure 37). These stations have a rather symmetric frequency distribution, where more than 40% of the summer days and about 30% of the total days have satellite derived global radiation within ±5% of the ground based value. This agrees with the low median relative differences for the total period (and for the summer period) which are 0.02 (0.00) for Karlstad and 0.04 (0.02) for Norrkoping.

Figure 38 shows the frequency distribution of the relative differences for the Swedish station Vaxjo. Combined with a shift towards positive values and a satellite derived overestimate, the frequency distribution is rather narrow for the total period and for the summer period. More than 20 % of the total days and 30 % of the summer days have satellite derived radiation within ±5% of the ground based value. Vaxjo has approximately the same percentages of total days and summer days where the satellite estimates are 5 to 15 % higher than the ground based value, as the percentages within ±5% of the ground based value. This is characteristic of Vaxjo.

During the total and the summer period, there is a slight shift towards negative values in the frequency distribution of relative differences between satellite derived and measured daily global radiation at Aas (figure 39). This is the only station with a shift towards negative values and has the only negative median relative difference (-0.01 during summer). Other stations have either an approximately symmetric frequency distribution, or a shift towards positive relative differences.

In figure 35, the frequency distribution of the relative satellite derived and observed global radiation difference at Kise for the years 1999 and 2000 are shown. Despite a large fraction of values equal to (or originally bigger than) 1.4 during winter, there is a shift towards negative values. Approximately 20 % the winter days have satellite derived global radiation that are 5 to 25 % lower than the ground based value. Also here it is a tail in the distribution, towards high positive relative differences.

Table 9 gives the percentage of satellite derived daily global radiation values within ±15% of the ground truth values, for the whole year and for summer and winter separately. Here, the difference between summer and winter is evident, with winter values approximately half of the summer values.

As shown in table 9, Karlstad and Norrkoping are the stations with the largest percentage of days where the satellite derived global radiation are within ±15% of the ground based value. For these stations, more than 80 % of the summer days and more than 60 % of the total days have satellite derived global radiation within ±15% of the ground based value. The corresponding percentage of values within ±5% are 40 % and 30 % (36 and 37). By increasing the limits from ±5% to ±15% , the fraction of days within the intervals for
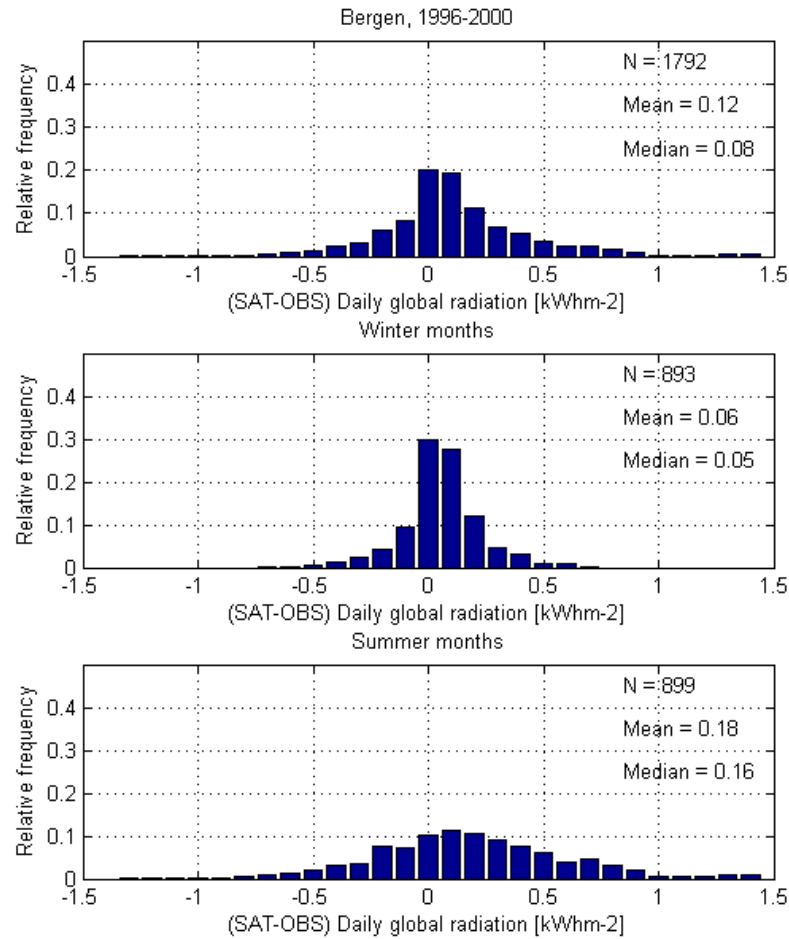
Figure 32: The frequency distribution of the actual difference between global radiation derived from METEOSAT data (SAT) and ground truth values (OBS) at Bergen during 1996-2000. This is done for the whole year (all years) in the top section of this figure, winter months (October-March, all years) in the middle and summer months (April-September, all years) at the bottom. Mean and median are given, and N is the total number of days plotted.
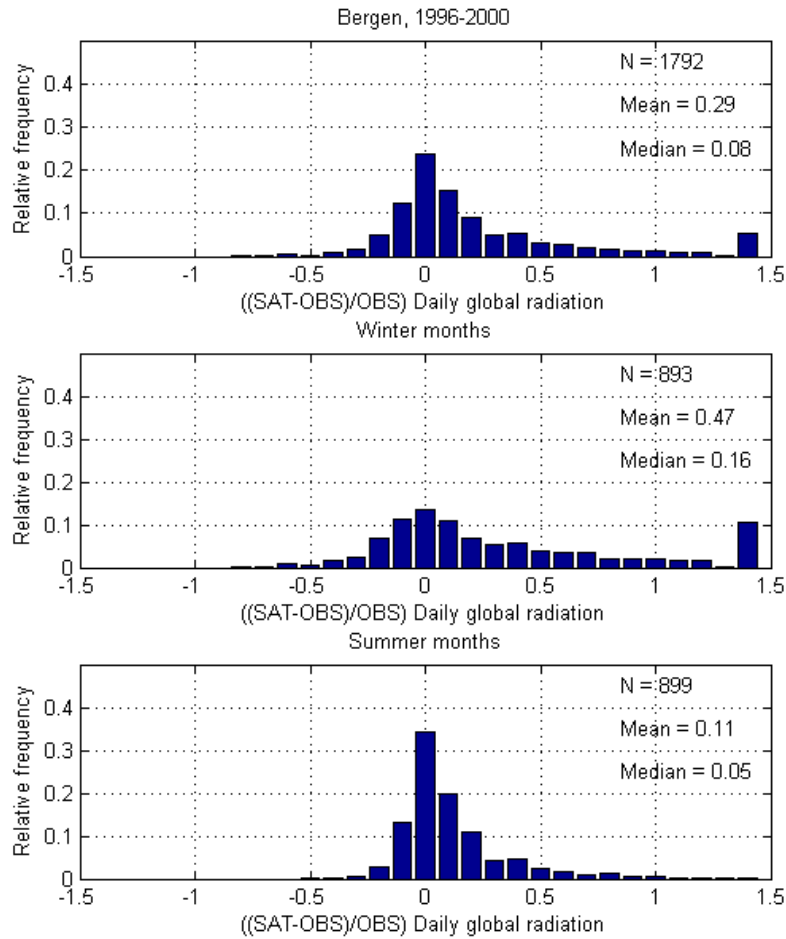
Figure 33: The frequency distribution of the relative difference between global radiation derived from METEOSAT data (SAT) and ground truth values (OBS) at Bergen during 1996-2000. This is done for the whole year (all years) in the top section of this figure, winter months (October-March, all years) in the middle and summer months (April-September, all years) at the bottom. N is the total number of days plotted and mean are the average values.
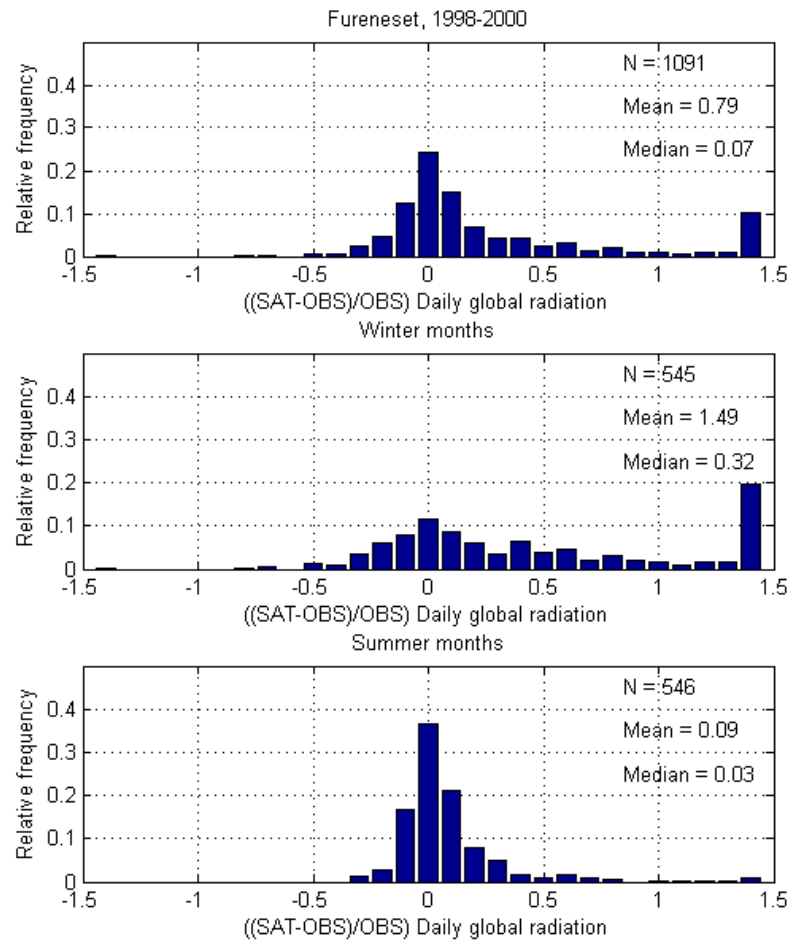
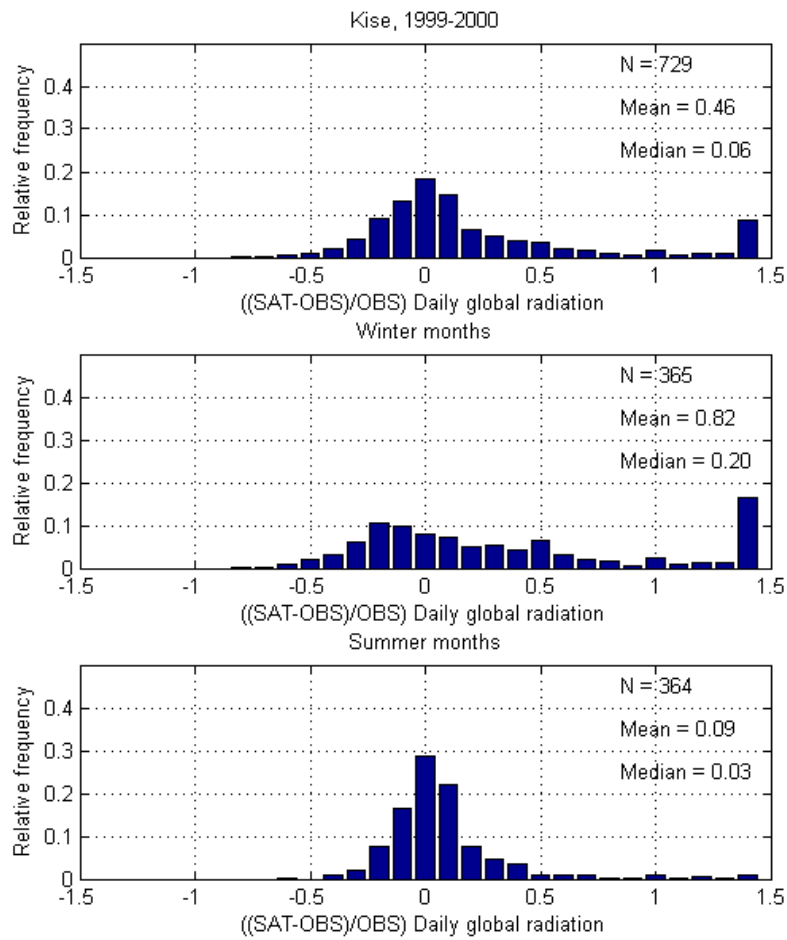Figure 34: Same as figure 33, for Fureneset and the years 1998-2000.

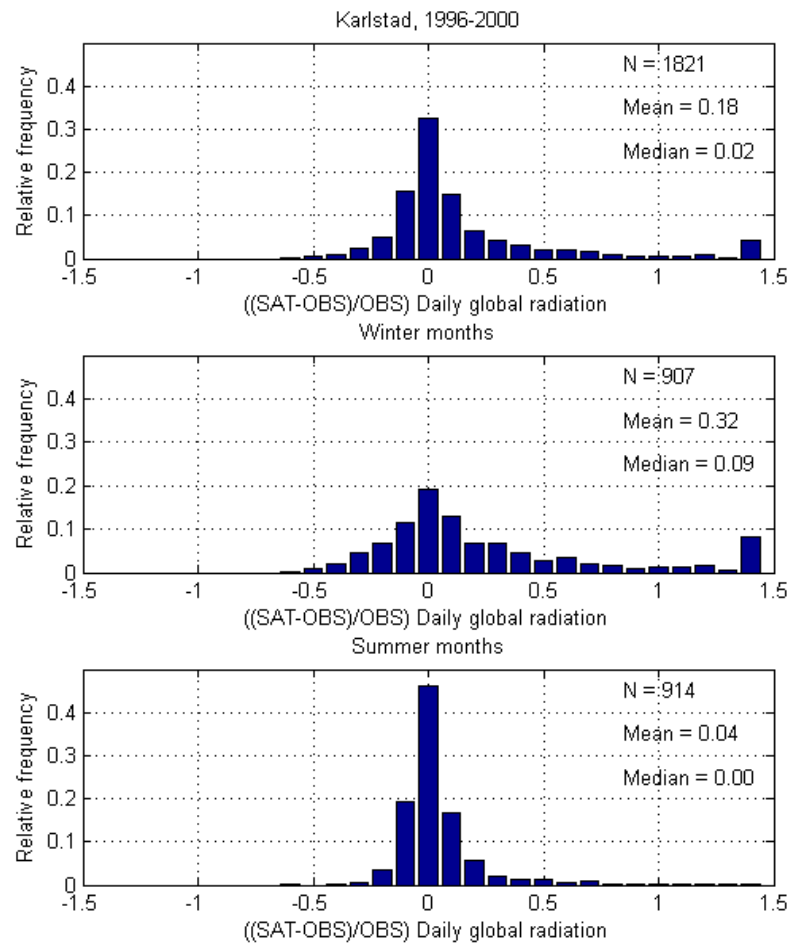Figure 35: The same as figure 33, for Kise and the years 1999-2000.
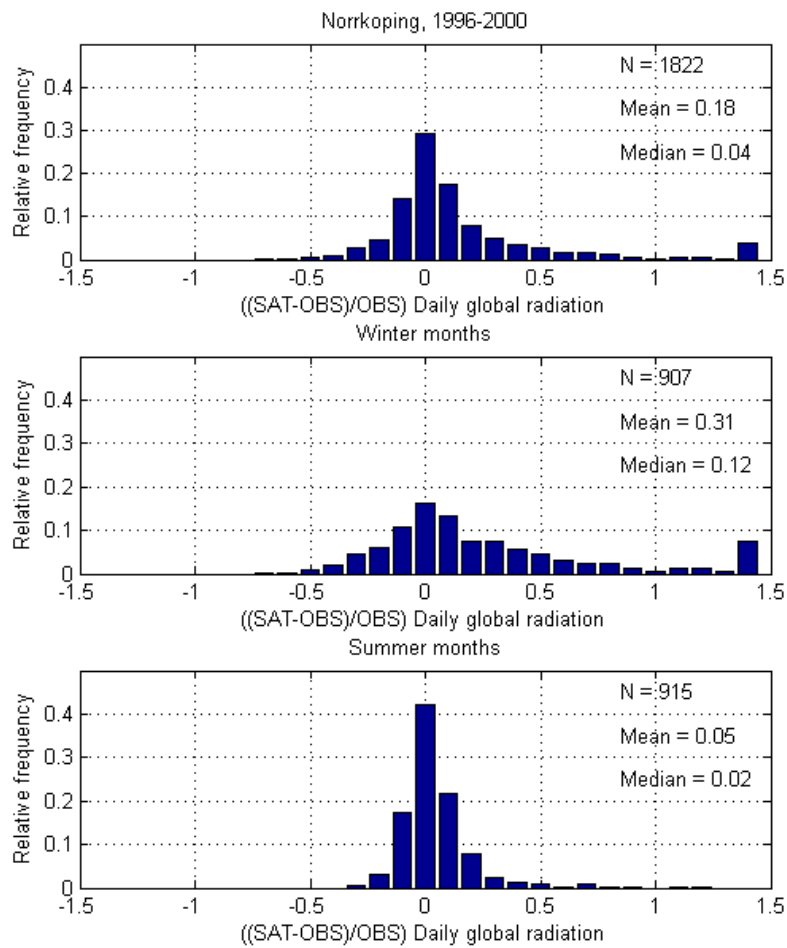
Figure 36: The same as figure 33, for Karlstad.
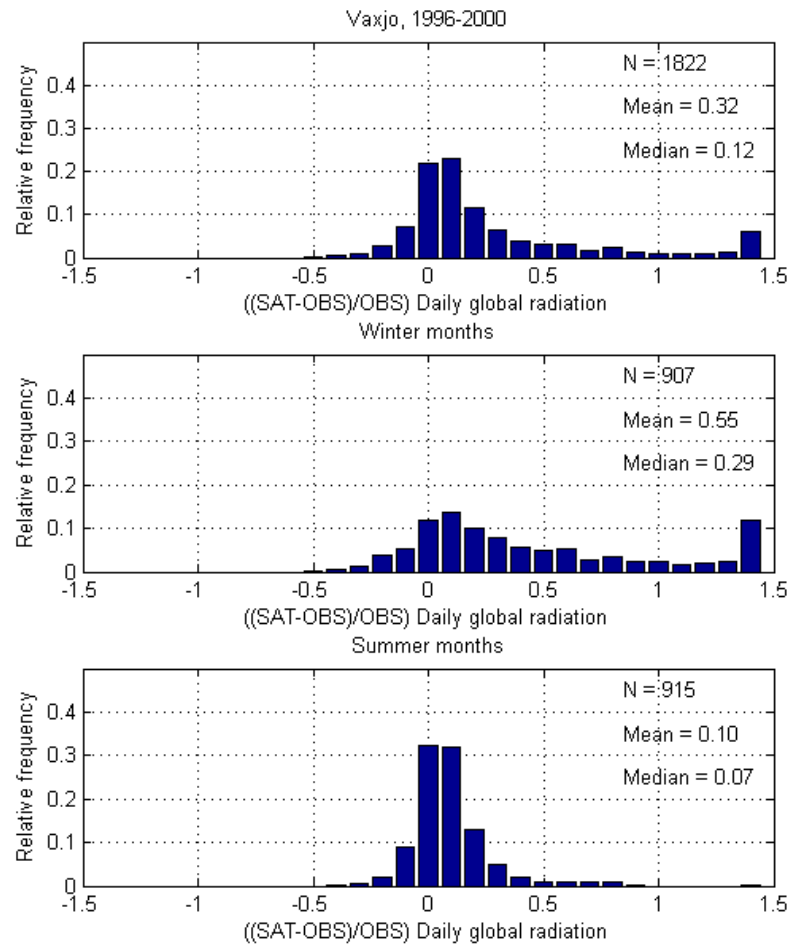
Figure 37: Same as figure 33, for Norrkoping.

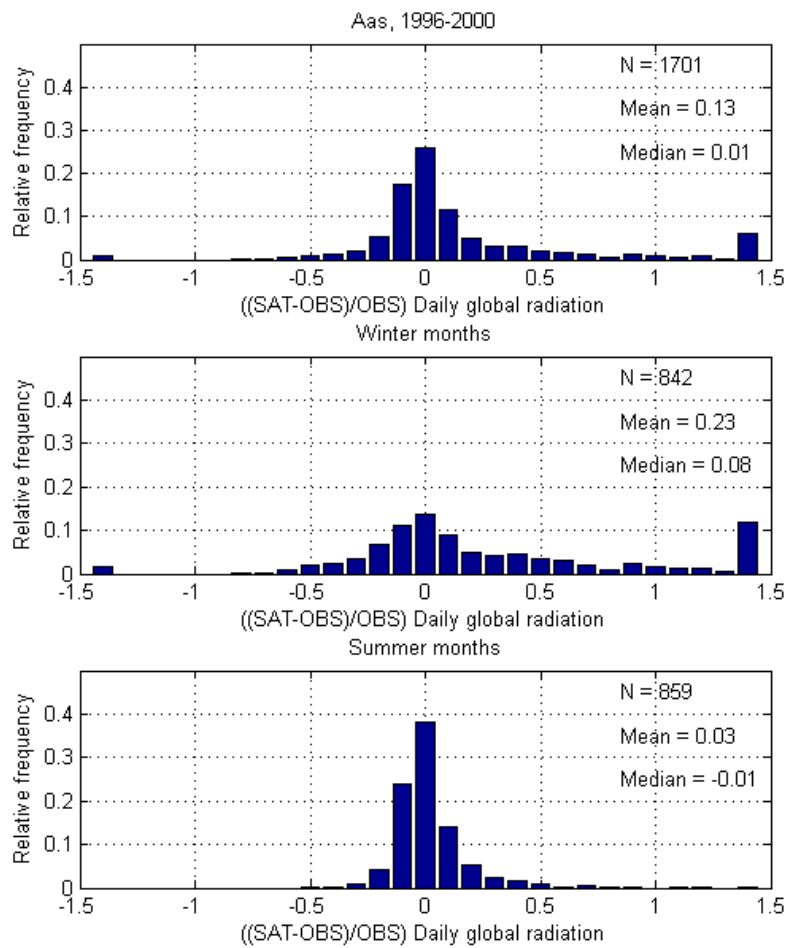Figure 38: The same as figure 33, for Vaxjo.

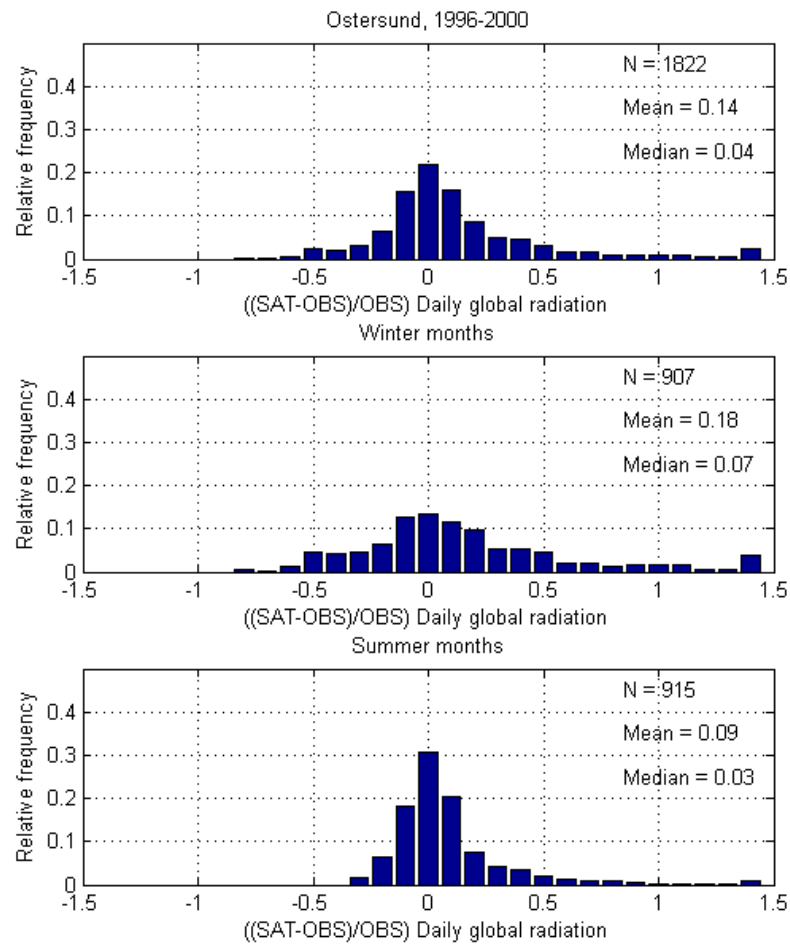Figure 39: The same as figure 33, for Aas.

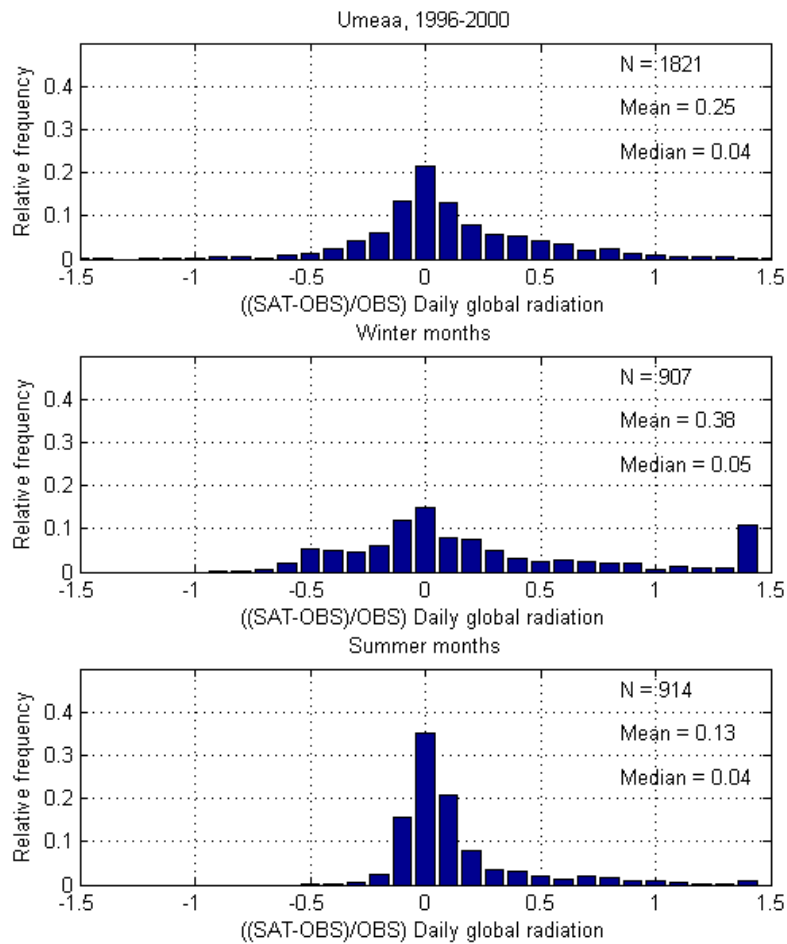Figure 40: Same as figure 33, for Ostersund.
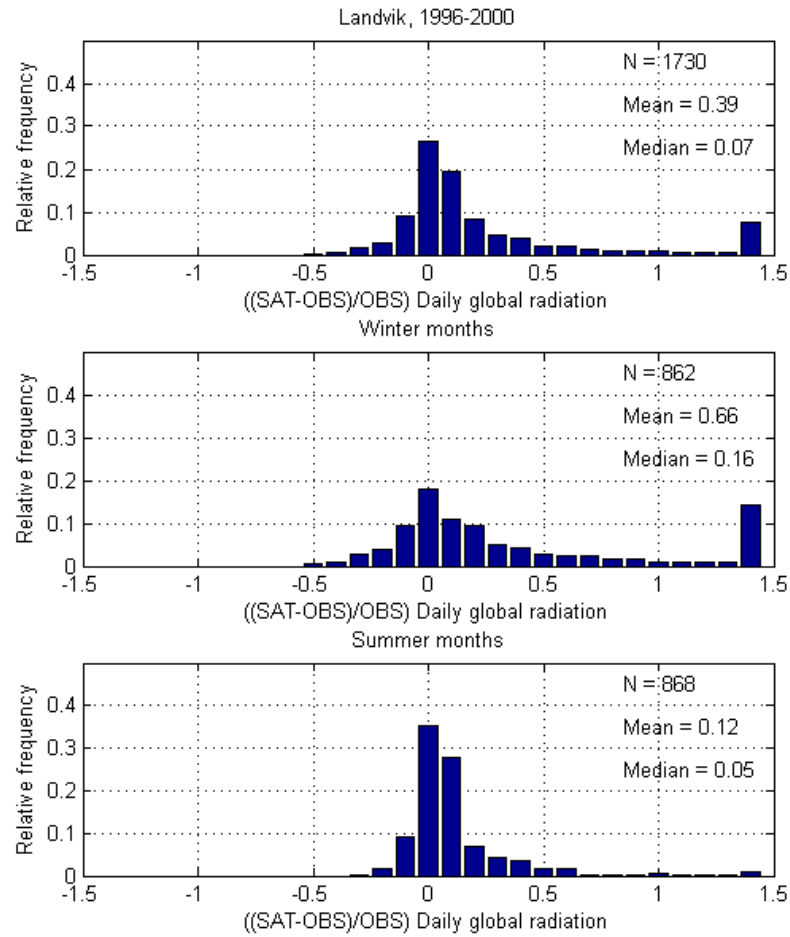
Figure 41: Same as figure 33, for Umeaa.

Figure 42: Same as figure 33, for Landvik.

Table 9: The percentage of satellite derived daily global radiation values within $\pm$ 15 % the ground truth value. Period indicates the years which the values are based on. Total includes the whole year, summer includes April-September and winter includes October-March.

Station	Period	Total [%]	Summer [%]	Winter [%]
Vaxjo	1996-2000	52.1	73.3	30.8
Landvik	1996-2000	55.2	72.1	38.2
Norrkoping	1996-2000	60.9	81.5	40.1
Karlstad	1996-2000	63.0	82.1	43.7
Aas	1996-2000	54.9	76.1	33.5
Bergen	1996-2000	51.3	66.8	35.8
Kise	1999-2000	46.0	66.9	25.0
Fureneset	1998-2000	51.3	74.3	28.2
Ostersund	1996-2000	53.6	69.3	37.8
Umeaa	1996-2000	52.9	71.3	34.5

Karlstad and Norrkoping are approximately doubled.

Kise has least agreement between satellite derived and ground based daily global radiation, according to table 9. For approximately 67 % of the summer days and 46 % of the total days the satellite estimated global radiation is within $\pm15\%$ of the measured value. The corresponding values within $\pm5\%$ of the ground based value (figure 35), were 30 % and 20 %.

For the other stations, approximately 50 - 55 % of the total days, 66 - 76 % of the summer days and 28 - 38 % of the winter days are within $\pm15\%$ of the measured value. Approximately twice as many days (percentage) are within the $\pm15\%$ limits during summer, compared to winter. This agrees with the results from plotting the frequency distribution of the relative differences between satellite derived global radiation and ground based global radiation for the season separately (figures 33 - 42). The values in table 9 are basically a summary of the results from figures 33 - 42.

4.2.2   The effect of snow-cover and horizon screening

Satellite derived solar radiation from the period 1996-2000 are readily available at the www server of the EU-project Satel-Light (Fontoynont et al. 1998) and provide results which corresponds well to their measured ground truth counterparts. As mentioned in chapter 3.3, the satellite interprets reflection of solar radiation from snow-covered ground as reflection from clouds and thus sees more clouds than it actually is. Normally, this causes an underestimation of the satellite derived global radiation.

The issue concerning separating snow from clouds is examined by plotting measured hourly global irradiance against the Meteosat counterparts. Since information about snow-cover is only available for the Norwegian sites, this is done for Bergen and Kise. Figure 43 shows the three cases 05.01.1996, 06.01.1996 and 10.02.1999 where the combination of snow-cover and sunshine duration close to 100 % of maximum sunshine duration occurs at Bergen. The similar situation occurs 06.02.1999, 16.02.1999 and 07.04.2000 at Kise, and this is shown in figure 44.

Note that the y-axis differs for figures 43 and 44, and also within the different sections in the former figure. To prevent the low curves in the two first situations in Bergen to be squeezed into the lower part of the figure and make it difficult to see the difference between the measured, modelled and satellite derived global radiation curves, the scale of the sections had to be different. Global solar radiation is considerable larger for months close to summer and consequently needs a y-axis with larger range.

The measured global radiation curve at a clear day in Bergen is very characteristic during winter months (see figure 43). Bergen is surrounded by mountains blocking the direct solar radiation for parts of the day (see figure 45). A distinct pattern where the sun disappears behind the horizon early in the afternoon during mid-winter is identifiable, both in the measured global radiation (fully drawn line) and modelled clear sky radiation (dotted line). Combined with small global radiation values during this season, maximum solar irradiance and sunshine duration are small.

Measured global radiation applied in this thesis are on an hourly basis. When these values, which in addition are low and few during winter, are plotted for Bergen, the global radiation curve will be quite uneven. The maximum solar elevation is low during winter at these latitudes and this results in few hours with contribution from the direct component. A steep increase in the global radiation curve after sunrise is followed by a sudden drop when the sun is reducing its altitude again.

For all three days in Bergen, the satellite gives too low values for the period where the sun elevation exceeds the horizon (figure 43). The main reason for this is that the satellite interprets high reflection from snow as clouds and thus overestimates the cloud fraction in equation 14 (given in section 3.3.1). The two first days had an approximately 30 cm deep snow-cover and the last day had a snow depth of approximately 15 cm. Here, it must be mentioned that the reflectivity value for Bergen is an average over a 3 * 5 pixel area (section 3.3), where pixels more or less over ocean are included in the

Figure 43: Hourly global irradiance at Bergen derived by the Heliosat procedure from
Meteosat data (dashed line) plotted versus their ground truth values (fully drawn line)
for 05.01 and 06.01 in 1996 and 10.02 in 1999. The modelled clear sky curve (dotted
line) is also given for each of the situations. The scale of the y-axis in the bottom section
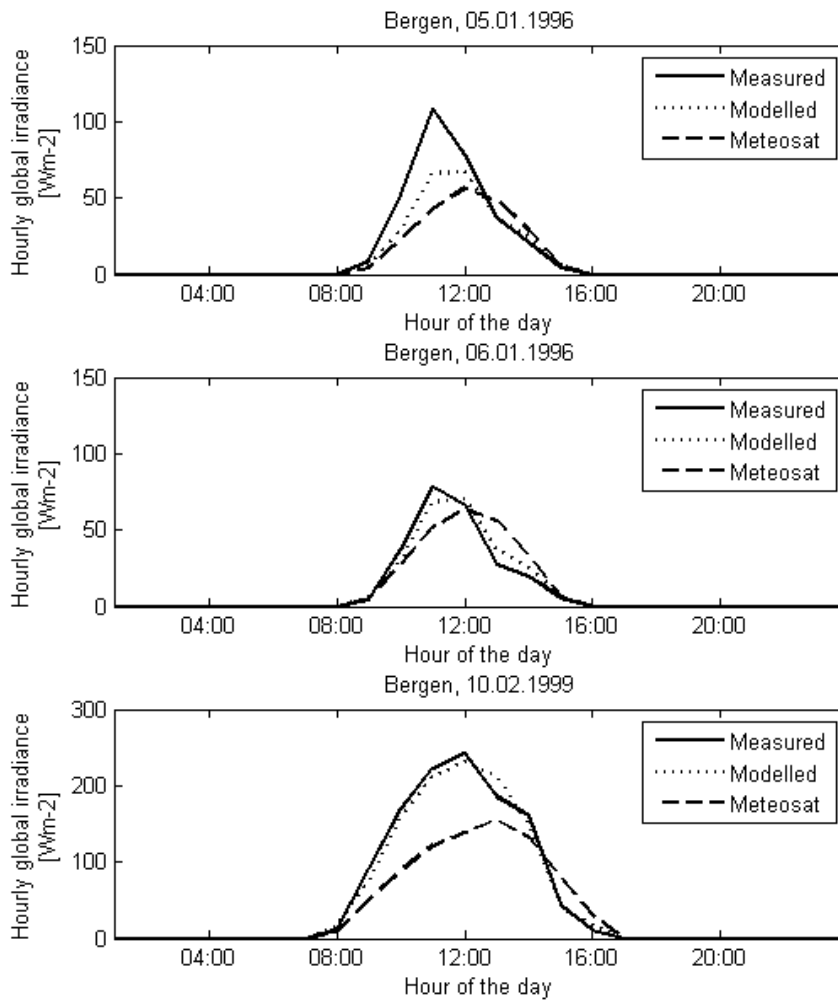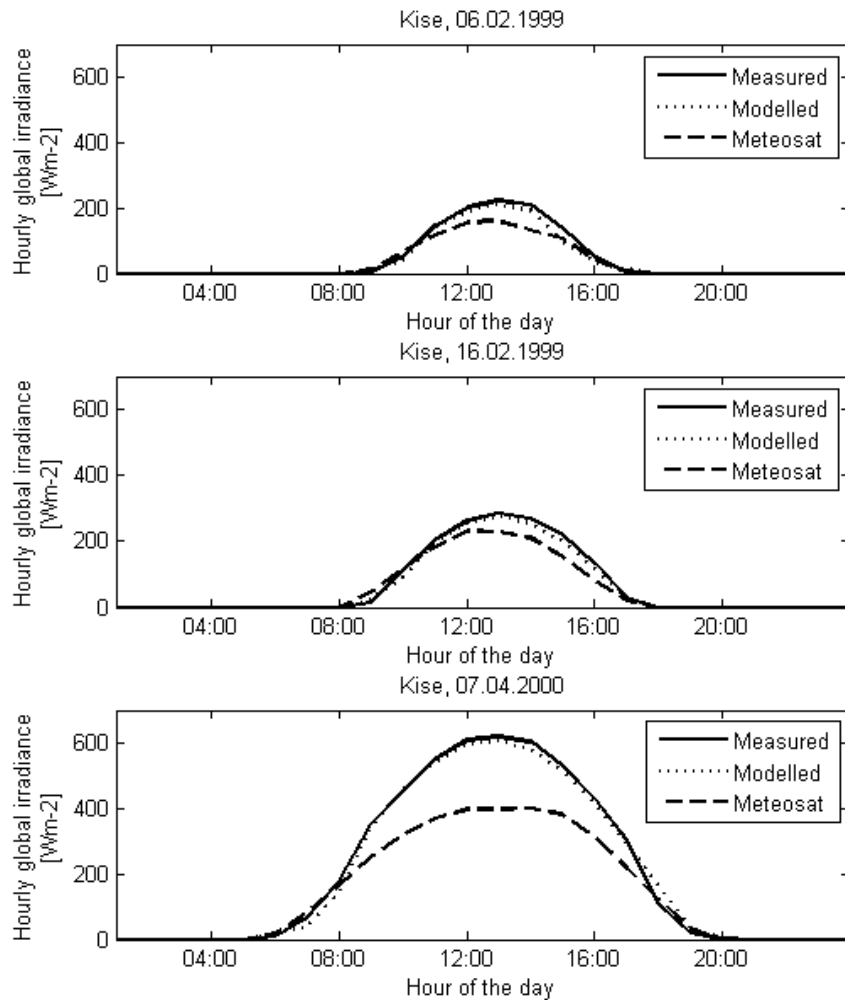is different from the two top sections.

Figure 44: Hourly global irradiance at Kise derived by the Heliosat procedure from Meteosat data (dashed line) plotted versus their ground truth values (fully drawn line) for 06.02.1996, 16.02.1996 and 07.04.2000. The modelled clear sky curve (dotted line) is also given for each of the situations. The scale of the y-axis is different from the scale in figure 43.

average. Pixels over ocean have a low reflectivity and will reduce the snow effect for the total area.

For the afternoon period with the sun below the horizon, Meteosat gives too high values, even though the satellite overestimates the cloud fraction. The main reason for this is that while the satellite has no information of the horizon (assumes no horizon screening), the measuring instruments will sense that the horizon will screen for the direct radiation.

There are differences between the three days in Bergen. While the two first days have approximately the same screening effect, the screening effect for the last day is much smaller (figure 45). Besides, there is a difference in measured global radiation between the two first days (figure 43). While the measured values agree quite well with the modelled clear sky values on January 6, the measurements exceed the modelled values substantially the day before. The reason for the high values on January 5 is not known; perhaps reflection from snow close to the instruments gives a contribution here. In addition, measuring errors can not be excluded for these low solar elevations ($< 7°$).

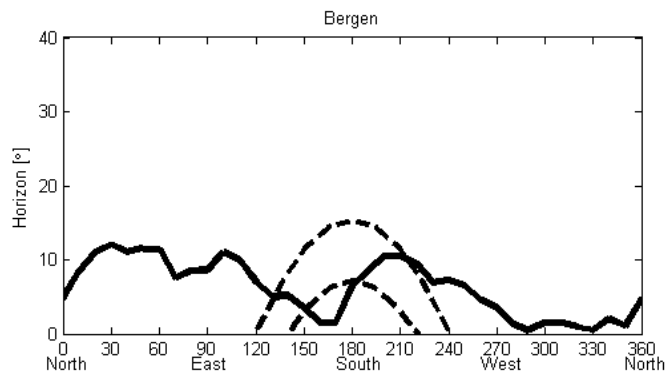Figure 45: Horizon panorama for Bergen. Thirty-six elevation angles in the directions from 10° to 360° azimuth are given. The solar path is indicated for January 6 (dashed lower curve) and February 10 (dashed upper curve). The sun path on January 5 is almost identical to the sun path on the day after and is omitted.

Like in Bergen, figure 44 shows that the satellite underestimates the surface global radiation in situations with snow-covered ground and sunshine duration close to the maximum sunshine duration also at Kise. The effect of the horizon is not as large as in Bergen, but at low solar elevations there is a slight overestimation of the satellite derived global radiation. Meteosat assumes no horizon and will therefore ignore the fact that instruments are not receiving any direct radiation when the sun is behind the topography.

As mentioned in chapter 3.3, the reflected global radiation is averaged over three pixels in latitude and five pixels in longitude. This means that the pixel is averaged over fifteen pixels. At the latitudes of Scandinavia, these pixels cover five kilometres in longitude and sixteen kilometres in latitude. The reflectivity is therefore averaged over an area
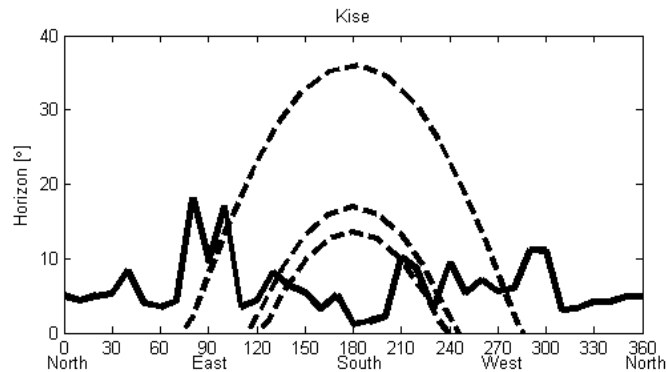
Figure 46: Horizon panorama for Kise. Thirty-six elevation angles in the directions from 10° to 360° azimuth are given. The solar path is indicated for February 6 (dashed lower line), February 16 (dashed middle line) and April 7 (dashed upper line).

covering twenty-five kilometres in longitude and forty-eight kilometres in latitude.

Figure 47 shows one example of the geographical range of the averaging area when estimating the global radiation at Kise. This station is situated away from the Norwegian coastline and at an peninsula almost surrounded by the large lake Mjoesa, which is also shown on figure 47. It does not exist information about exactly which area the satellite is averaged over, so it is not known how large fraction the lake Mjoesa constitute of the pixel.

The reflected solar radiation from Mjoesa measured by the satellite depends on the albedo of the lake. Table 1 (section 2.2) shows that the albedo of an ice-covered surface covered is larger than an unfrozen water surface. Observations of the ice-cover of Mjoesa exist and show that it was frozen from January 29 to May 1 in 1999 and open during 2000 (Sandberg 2011). This means that the two first situations in figure 44 most probably are averaged over a snow-covered lake, while the last situation consists of an unknown fraction of reflection from a water surface. Nevertheless, figure 44 shows that the underestimation is largest for the last situation (April 7, 2000). Here it must be mentioned that there is no information about the snow-cover in the surroundings of the station Kise. Forest without snow or forest with surface snow cover in the surrounding area, have low albedo (see table 1 in section 2.2) and might reduce the reflectivity of the pixel and the snow-effect.

As discussed in this section, snow-covered ground and horizon has the opposite effect on the hourly global radiation. The former increase the surface reflectivity (and consequently the satellite estimated cloud amount), while the latter might block the direct solar radiation received by the pyranometers for parts of the day. The result is an underestimated satellite derived global radiation when the sun is above the horizon and an overestimated satellite derived global radiation when the sun is behind the horizon. In some cases these two effects will compensate for each other in the daily sums. One

Figure 47: The geographical range which one pixel potentially can be averaged over. The black dot on the peninsula indicate where Kise is located. The map is downloaded from *Google Maps, a web mapping service application provided by Google* (n.d.).

example is Bergen on January 6 (figure 43), where the measured daily global radiation is 240 Wh/m^2 and the satellite derived daily global radiation is 246 Wh/m^2.

4.3 Spatial variation of average global radiation

The mean daily global radiation derived from Meteosat data are compared to the ground truth data for all stations (except Skogmo because of poor data quality) and presented in figure 48. This daily average global radiation is computed from daily global radiation values from five years (1996-2000) at stations with data for the whole period which is approved by the quality control. Kise and Fureneset have two and three years with good measurements, respectively, and data for the periods 1999-2000 and 1998-2000 constitute the basis for the averages.
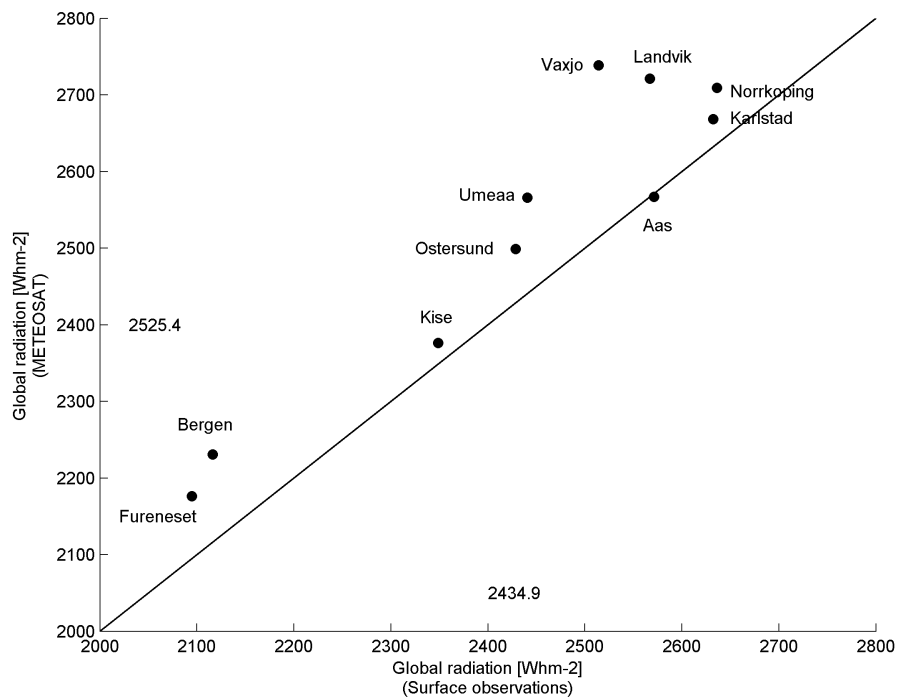

Figure 48: Average daily values of ground truth and Meteosat derived global radiation for ten Scandinavian stations. The 1:1 line is indicated and the number of days forming the basis of the averages for each station are given as N in table 8 (in section 4.2). Averages for all ten stations are given as numbers (in Wh/m^2).

According to table 8 and figure 48, Fureneset and Bergen have annual daily global radiation averages between 2050 Wh/m^2 and 2150 Wh/m^2. Also here, data from these two westernmost stations differ from data at the other stations by being lowest (bottom left corner figure 48). As for almost all stations except from Aas (below the 1:1 line in figure 48), the satellite also overestimates the ground truth values at Fureneset and Bergen according to the annual daily averages.

Stations south and east of the Scandinavian mountain range (top right corner figure 48)

have approximately larger averages than stations on the western side. Vaxjo, Landvik, Aas, Norrkoping and Karlstad are situated at low latitudes and have annual daily averages from approximately 2500 Wh/m^2 to 2700 Wh/m^2. Umeaa, Ostersund and Kise have annual daily global radiation average from approximately 2350 Wh/m^2 to 2450 Wh/m^2 (central parts of figure 48).

The three stations Bergen, Aas and Karlstad are all located at about 60°N and have five years of data each. According to figure 48, they have annual daily averages reaching from about 2100 Wh/m^2 for Bergen to around 2700 Wh/m^2 for Aas and Karlstad. The main reason for these differences is different cloud amount/type, and the figure shows that the differences are nicely picked up by the satellite.

As an average for all the stations, the annual MBD is less than 4% (figure 48), while for each of the individual stations MBD is less than 9% (table 8). This is the case for all the Scandinavian stations, including the northernmost, southernmost and stations on both sides of the mountain chain. This corresponds with the results which Olseth & Skartveit (2001) found for the years 1996 and 1997 for some Norwegian stations.

5   Summary and conclusions

The solar radiation climate of Scandinavia is studied. Daily global radiation data for the stations Vaxjo, Landvik, Norrkoping, Karlstad, Aas, Bergen, Kise, Fureneset, Ostersund, Umeaa and Skogmo from the five years 1996-2000 constitute the basis for this thesis. These stations are mainly situated along the west and east coast of the Scandinavian Peninsula, but some can be found at locations further inland.

One of the tasks of this work is to perform a quality control of the daily global radiation at eleven stations. To do this, modelled clear sky global radiation was produced by running the McMaster model described by Davies & McKay (1982). Climatological averages of water vapour and ozone are input parameters. Preferable, the horizon panorama is also needed. Information about the horizon elevation was only available at the Norwegian stations. It is especially important for stations with tall mountains in the surroundings, which is not a rarity in western parts of Scandinavia.

To control the quality of the global radiation data, measured and modelled daily values were compared. This was done by directly comparing the corresponding values and by analysing the frequency distribution of clear sky indices. These clear sky indices represent the ratio of measured global radiation and modelled clear sky global radiation. Generally, the estimated clear sky values coincide with the highest measured values for the whole period. Some exceptions are 1996-1997 at Fureneset and 1996-1998 at Kise. Instrument error causes outliers and negative values in the former case, while the highest observed global radiation values are lower than the modelled clear sky curve for the latter. In addition, the measurements at Skogmo are discarded by the quality control due to poor data quality. If ranking the average clear sky index at each station from large to small, Umeaa has the largest (based on data from 1996-2000) and Fureneset has the smallest (based on data from 1998-2000) average clear sky index and thus the smallest and largest cloud amount, respectively.

Fureneset, Bergen and Vaxjo have turned out to be the stations with the lowest mean clear sky indices. The two former stations are located at the west coast of Norway and the latter is located inland at the southern part of Sweden. For a five year period (1996-2000), Bergen has average clear sky index equal to 0.545 and Vaxjo has 0.554. If considering the average clear sky index for the years 1998-2000 (which the station Fureneset has data with approved quality from), the corresponding values are 0.503, 0.517 and 0.533 for Fureneset, Bergen and Vaxjo, respectively. By excluding the two first years from the basis of the averages for Bergen and Vaxjo, the values are reduced. This might imply that 1996 and 1997 are years with less clouds than the last three years.

The frequency distribution of the clear sky indices for Ostersund and Umeaa was presented for summer and winter seasons separately. For the total period where all months were included, the mean clear sky indices were approximately 0.689 and 0.691, respectively. A distinct tail of large values was also detected for both stations. By considering the seasons separately, the result was lower summer averages at both Ostersund (0.651)

and Umeaa (0.670) and higher winter averages for Ostersund (0.804) and Umeaa (0.798). The tail of large values was identified as a winter phenomenon by this seasonal division.

Stations as Aas, Kise, Landvik, Karlstad and Norrkoping have average clear sky indices in the range 0.580 - 0.631. Here, it is important to note that the average at Kise is based only on data from 1999 and 2000, while the four other stations have approved data from the whole period (1996-2000). As shown for Bergen, there might be variations in average clear sky index from year to year. By only considering the two last years for all these stations, minor changes in the averages are identified.

Measured global radiation is also compared to satellite derived global radiation. The Satel-Light team estimated the latter from Meteosat data by using a modified Heliosat method, which originally was presented by Cano et al. (1986). The geostationary satellite Meteosat measures the reflected solar radiation and calculates a cloud index from this. Increased reflection is interpreted as increased cloud amount by the satellite.

Daily global radiation values estimated by the satellite were compared to their ground truth counterparts for ten stations. Generally, the daily estimates are good. For all stations except Aas, the satellite slightly overestimates the surface global radiation. By calculation of the MBDs and RMSDs of the difference between satellite derived global radiation and ground truth data, it was found that MBDs varies from slightly negative (-1%) to approximately 9%, while RMSDs varies from approximately 12% to 19%.

Satellite derived hourly global irradiances were also plotted against the ground truth counterparts, but only for Bergen. The hourly values are more scattered around the 1:1 line than the daily values. By analysing the mean hourly values for different solar elevations, the resulting small averages indicate a large fraction of small hourly irradiances for all the solar elevations, but especially for low solar elevations ($< 15°$). In addition, there is a trend of overestimation for low hourly values and a trend of underestimation for larger hourly values. Overall the satellite gives good estimates of global radiation, but there are some differences between cloudy and clear sky situations.

The best agreement between satellite derived and ground based daily global radiation appears for the Swedish stations Karlstad and Norrkoping. They have low median relative differences and a rather symmetric frequency distribution, where as much as approximately 40% of the summer days and 30% of the total days have satellite derived global radiation within $\pm 5\%$ of the ground based value. The similar values for summer and total days with satellite estimate within $\pm 15\%$ of the measured value are more than 80% and 60%, respectively. In addition to these large percentages, they also have among the lowest MBD and RMSD. For both Karlstad and Norrkoping, MBDs and RMSDs are below 3% and below 13%, respectively.

Kise is the station with least agreement between satellite derived and ground based daily global radiation. Approximately 30% of the summer days and 20% of the total days have satellite derived global radiation within $\pm 5\%$ of the ground based value. Despite a low MBD (approximately 1%), Kise has the largest RMSD with 19%. It is important to

77

note that these values are based on data from the two years 1999-2000, compared to the other stations (except Fureneset) with data from the five years 1996-2000.

During winter, the ground is periodically covered by snow at the latitudes of Scandinavia. Snow increases the reflected solar radiation from the surface. This increased reflectivity, is interpreted as solar radiation reflected from clouds by Meteosat. Increased reflection from clouds and consequently an increased estimated cloud amount reduces the satellite derived surface global radiation. Clear sky situations with snow-covered ground at the two Norwegian stations Bergen and Kise have shown to experience too low satellite derived global radiation.

Some Scandinavian stations are surrounded by mountains. If this is the case, topography might block the direct component of the global radiation for periods of the day, causing a reduction in the measured global radiation and in the modelled clear sky radiation (if horizon panorama is available). Satellites have no information about the horizon and ignore the effect of the topography on the radiation. This results in an overestimated global radiation during hours when the sun is below the actual horizon. The effect of the horizon is present especially at low solar elevation for both Bergen and Kise, but is largest at Bergen.

The effect of horizon screening and snow-cover are opposite, and might compensate for each other when comparing daily measured and satellite derived global radiation. The horizon blocks the direct component of the solar radiation for parts of the day, while snow-cover increase the surface reflectivity and thus the satellite estimated cloud amount. As seen for Bergen on January 6 (1996), the underestimated global radiation caused by the snow effect counterbalances the overestimated global radiation caused by the effect of the missing information about the topography. The measured daily global radiation in this situation is 240 Wh/m^2 and the satellite derived daily global radiation is 246 Wh/m^2, despite differences in the values for individual hours.

A comparison of annual mean daily global radiation shows a spatial variation. Stations situated on the west side of the Scandinavian Peninsula (Fureneset and Bergen) have lower averages than stations further east. As example, Bergen, Kise and Karlstad are located at nearly the same latitude (60°N), ranges from approximately 5°E to 13°E in longitude and have averages between approximately 2100 Wh/m^2 and 2700 Wh/m^2. Different cloud amount/type is mainly the reason for the differences in the averages for these stations, and this is nicely picked up by the satellite.

On the basis of a five year period, daily solar radiation data for eleven stations on the Scandinavian Peninsula have been studied. The stations are situated at relatively high latitudes and have some climatologically differences. In addition to giving an overview of the solar radiation climate of these high latitudes, the analysis of results from comparing satellite derived global radiation and ground truth data is a large part of this work. The geostationary satellite measuring the reflectivity is constantly overlooking the same surface area, but at an unfavourable angle at these latitudes. In addition, quality control has also shown to be important when working with solar radiation data.

A   First appendix: Statistics

Mean bias deviation

To describe the performance of the model which derive global solar radiation from satellite data, we use a quantity called Mean bias deviation (MBD). This quantity is defined as

$$MBD = 100\frac{\frac{1}{n}\sum_1^n(model - measurement)}{\frac{1}{n}\sum_1^n(measurement)} \tag{17}$$

where n is the size of the estimated parameter and corresponding measurements. Multiplication by 100 gives percent. The quantity characterize the bias of the model. Negative values if the model underestimates and positive if the model overestimate.

Root mean square deviation

Another quantity used to characterize the bias of a model is the root mean square deviation (RMSD), which is defined by the formula

$$RMSD = 100\frac{\sqrt{\frac{1}{n}\sum_1^n(model - measurement)^2}}{\frac{1}{n}\sum_1^n(measurement)} \tag{18}$$

where n is the size of the parameter, as in the formula above. Multiplication by 100 gives percent.

A   Second appendix: Horizon panorama

This appendix contains the horizon panorama for the Norwegian stations Bergen, Kise, Landvik, Aas and Fureneset.
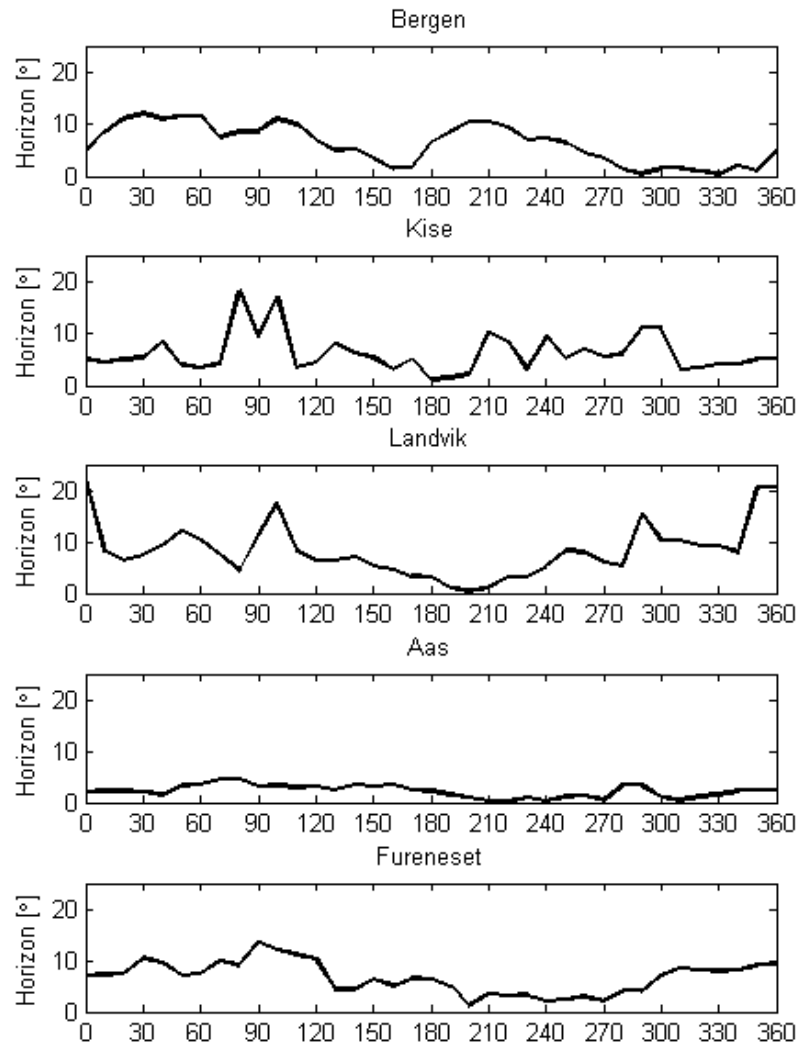

Figure 49: Horizon panorama for the Norwegian stations Bergen, Kise, Landvik, Aas and Fureneset. Thirty-six elevation angles in the directions from 10° to 360° azimuth are given.

References

Bairstow, A. (n.d.), 'Solar Geometry, Solar Radiation and Solar Control, in introductory lecture', http://www.l-e-s-s.co.uk/Guides/Physics/SolarGeometry.htm.

Beyer, H., Costanzo, C. & Heinemann, D. (1996), 'Modifications of the Heliosat procedure for irradiance estimates from satellite images.', *Solar Energy* **56**(3), 207–212.

Bioforsk (n.d.), http://www.bioforsk.no. The homepage of the Norwegian Institute for Agricultural and Environmental Research.

Cano, D., Monget, J. M., Albuisson, M., Guillard, H., Regas, N. & Wald, L. (1986), 'A method for the determination of the global solar radiation from meteorological satellite data.', *Solar Energy* **37**(1), 31–39.

Davies, J. & McKay, D. (1982), 'Estimating solar irradiance and components.', *Solar Energy* (1), 55–64.

Dumortier, D. (1995), Mesure, analyse et modélisation du gisement lumineux. Application à l'évaluation des performances de l'éclairage naturel des bâtiments., PhD thesis, Universite de Savoie, France.

eKlima, a web portal which gives free access to the climate database of the Norwegian Meteorological Institute (n.d.), http://eklima.met.no/.

Fontoynont, M., Dumortier, D., Heinemann, D., Hammer, A., Olseth, J. A., Skartveit, A., Ineichen, P., Reise, C., Page, J., Roche, L., Beyer, H. G. & Wald, L. (1998), 'Satellight', http://www.satel-light.com. A www server which provides high quality daylight and solar radiation data for western and central Europe. Proc. 9th Conference on Satellite Meteorology and Oceanography in Paris.

Google Maps, a web mapping service application provided by Google (n.d.), http://maps.google.no/.

Hartmann, D. L. (1994), *Global Physical Climatology*, Vol. 56, 1 edn, Academic Press.

Iqbal, M. (1983), *An introduction to solar radiation.*, Academic Press, Orlando, Florida.

Kasten, F. (1996), 'The linke turbidity factor based on improved values of the integral rayleigh optical thickness.', *Solar Energy* **56**(3), 239–244.

Kipp & Zonen (2000), 'Instruction manual CM11 Pyranometer'.

National oceanic & atmospheric administration (NOAA). (n.d.), 'Solar Calculator Glossary', http://www.srrb.noaa.gov/highlights/sunrise/glossary.html.

Olseth, J. A. & Skartveit, A. (1989), 'Observed and modelled hourly lumnious efficacies under arbitrary cloudiness', *Solar Energy* (3), 221–233.

Olseth, J. A. & Skartveit, A. (2001), 'Solar irradiance, sunshine duration and daylight illuminance derived from Meteosat data for some European sites', *Theoretical and Applied Climatology* (3–4), 239–252.

Olseth, J., Skartveit, A. & Skaar, E. (1996), 'Retrospective quality control of solar radiation data', Second SATELLIGHT meeting, Bergen.

Page, J. (1996), 'Algorithms for the satellight programme.', Technical Report for the Second SATELLIGHT meeting, Bergen, Norway.

Paltridge, G. W. & Platt, C. M. R. (1976), *Radiative processes in meteorology and climatology*, Elsevier Scientific Publ. Comp., New York.

Perez, R., Ineichen, P., Seals, R., Michalsky, J. & Stewart, R. (1990), 'Modeling daylight availability and irradiance components from direct and global irradiance.', *Solar Energy* **44**(5), 271–289.

Rohde, R. A. (2007), 'Solar Radiation Spectrum, created for Global Warming Art.', http://www.globalwarmingart.com/wiki/File:Solar_Spectrum_png.

Sandberg, E. (2011), Personal communication.

smhi.se, the on-line climate database of the Swedish Meteorological and Hydrological Institute (n.d.), http://www.smhi.se/.

Utaaker, K. (1991), *Mikro- og lokalmeteorologi*, 1 edn, Alma Mater Forlag.

Wanielista, M. P., Kersten, R. & Eaglin, R. (1997), *Hydrology: water quantity and quality control*, 2 edn, John Wiley and Sons.

yr.no, which is an on-line weather service by the Norwegian Meteorological Institute and the Norwegian Broadcasting Corporation (NRK) (n.d.), http://www.yr.no/.

Zelenka, A., Perez, R., Seals, R. & Renne, D. (1999), 'Effective accuracy of satellite-derived hourly irradiances', *Theoretical and applied climatology* **62**(3–4), 199–207.